Spring 2023

# Advancing a Design for Trusted Community Bathymetry

Daniel Tauriello
*University of New Hampshire, Durham*

# ADVANCING A DESIGN FOR TRUSTED COMMUNITY BATHYMETRY

By

Daniel G. Tauriello

Bachelor of Science in Marine, Estuarine and Freshwater Biology, University of New Hampshire, 2014

THESIS

Submitted to the University of New Hampshire
In Partial Fulfillment of
The Requirements for the Degree of:

Master of Science
In
Earth Science: Ocean Mapping

May 2023

# Committee

This thesis was examined and approved in partial fulfillment of the requirements for the degree of Master of Science in Earth Science: Ocean Mapping:

**Thesis Director, Brian Calder,**
Research Professor of Ocean Engineering

**Semme Dijkstra,**
Clinical Professor, Center for Coastal and Ocean Mapping

**Andrew Armstrong,**
Affiliate Professor of Ocean Mapping

Approval signatures are on file with the University of New Hampshire Graduate School.

# Dedication

This thesis is dedicated to the late Captain Ben Smith, who inspired me to believe that everything is possible with the right dose of gumption.

# Acknowledgements

This work is fully funded by NOAA grant NA20NOS4000196.

# Table of Contents

Advancing a design for trusted community bathymetry ..... i
Committee ..... iii
Dedication ..... iv
Acknowledgements ..... iv
Table of Contents ..... v
Abstract ..... viii
Introduction ..... 1
Background ..... 1
Prior Work ..... 5
Motivation ..... 10
Contribution ..... 13
Chapter 1: Evaluating the Harxon GPS500 Antenna ..... 15
1.1 Introduction ..... 15
1.2 Methods ..... 16
1.3 Results ..... 19
1.4 Discussion ..... 23
1.5 Conclusion ..... 23
Chapter 2: Reverse Engineering the Garmin GCV-10 Side Scan Module ..... 24
2.1 Introduction ..... 24
2.2 Structure of a Garmin Installation ..... 25
2.3 Methods for Network Protocol Analysis ..... 26

2.4 Control Data Stream ........................................................................................ 28

2.5 Image Data Stream ........................................................................................... 30

2.6 Conversion to XTF Format ................................................................................ 33

Chapter 3: Integrating the Garmin GCV-10 with a TCB Datalogger ............................. 35

3.1 Introduction ....................................................................................................... 35

3.2 Logging Side Scan Data with the TCB Datalogger ............................................... 36

3.3 Optimizing Sidescan Range ............................................................................... 37

3.4 Determining the System Latency ........................................................................ 41

3.5 Autonomously Imaging Sidescan Targets in the Field ......................................... 48

3.5.1 Hardware Installation ....................................................................................... 48

3.5.2 Field Testing Latency Compensation ................................................................ 53

3.5.3 Demonstrating a Concept for Autonomous Operation ........................................ 58

Conclusions ............................................................................................................. 74

4.1 Implications of This Work .................................................................................. 74

4.2 Recommendations for Future Work .................................................................... 77

List of References ..................................................................................................... 80

Appendix A .............................................................................................................. 82

Table of Software ..................................................................................................... 82

Data Volume Experiment .......................................................................................... 83

Appendix B .............................................................................................................. 84

Logging Side Scan Data with the TCB Datalogger ..................................................... 84

Physical Installation .................................................................................................. 84

Software Installation ................................................................................................. 85

Echosounder Data Capture ........................................................................................85

Desktop Latency Experiment Procedure ...................................................................... 86

Processing Desktop Latency Experiment Data:......................................................................87

Processing Data from Field Collection........................................................................... 88

# ABSTRACT

The design for a Trusted Community Bathymetry (TCB) system, presented in Calder et al., 2020, demonstrates a data collection system capable of collecting precisely geo-referenced depth soundings from any navigational echosounder installed on a volunteer vessel. The TCB system is capable of autonomously determining any vertical installation offset with respect to the waterline, and provides sufficient guarantees of data quality to allow the soundings to be considered for hydrographic use.

This thesis presents two contributions to advance the original TCB system design. First, it capitalizes on the widespread availability of low-cost sidescan modules in the recreational sonar market by describing a method to integrate one of these units with the existing TCB datalogger. This integration adds significant richness to a volunteer dataset by enabling a hydrographic office to benefit from imagery of targets and obstructions in the vicinity of TCB vessels. Additionally, a method for autonomous operation is presented in which the TCB datalogger may command the sidescan to automatically log imagery in the vicinity of targets of interest specified by the hydrographic office.

Second, this work demonstrates it is possible to replace the survey-grade GNSS receiver antenna used in the original system design with a comparatively inexpensive unit. The replacement antenna does not provide equivalent real-time performance but can collect observations which can be post-processed to produce solutions with uncertainties on the same order as the survey-grade antenna. Since real-time performance is not important in a TCB application, this development represents a significant reduction in total system cost and increases the viability of widespread deployment without sacrificing data quality.

# INTRODUCTION

## Background

Hydrographic Offices (HO) are charged with charting vast tracts of navigable water, and subsequently publishing chart updates to ensure that hazards to navigation are clearly defined. However, maintaining large bathymetric datasets is not trivial, as it requires significant time and skilled labor to re-survey even a small geographic area. Due to the nature of this work, typically HO's are government agencies, such as the NOAA Office of Coast Survey (USA), or Canadian Hydrographic Service (CA). At current funding levels, HOs often lack the resources to comprehensively survey their authorized areas on a regular basis and must allocate their limited resources to prioritized survey zones. As a natural response, the international hydrographic community has long developed procedures for augmenting their datasets by sourcing depth soundings from non-hydrographic vessels.

Collecting bathymetric data from non-hydrographic vessels of opportunity is not a new concept in the hydrographic industry. Mariners have embraced a variety of platforms for sharing sensor data and observations to improve navigational safety and raise alert to hazards. Private companies including, Olex, Navionics, SeaID, TeamSurv, and Rose Point Navigation Systems, have incorporated or exclusively provided platforms for users to compile and share sensor data for decades (Hoy & Calder, 2019). This type of data will be referred to as Volunteered Geographic Information, or VGI. VGI has proven valuable in the maritime community, with sustained user-bases interested in the bathymetric and habitat-mapping products made available (Hoy & Calder, 2019). However, VGI often lacks the metadata and transparency in processing techniques essential to determining the uncertainty associated with the data reported. Since HO's retain legal liability for data portrayed on the chart, they have remained understandably conservative in incorporating volunteered depth data without robust means of empirical qualification.

Employment of a traditional crowdsourcing approach may offer a solution to dealing with the uncertainties associated with volunteered soundings. The concept of "crowd-sourced" bathymetry (CSB), relies on the assumption that if enough users make the same measurement, the average solution is an unbiased estimation of the truth. This phenomenon is often referred to as "the wisdom of the crowd" (Howe, 2008). In a practical sense, this implies that if many ships measure the depth of the same bathymetric feature, errors in sensor installation, calibration, vessel motion, sound speed, etc., will average out and the *true* depth will be determined.

A fundamental problem with implementing a crowdsourcing approach in the marine environment is that the ocean is large, and ships are relatively small. Therefore, the likelihood that many vessels pass over the same feature is low; an issue that is even more pronounced outside of high traffic areas and commercial shipping lanes. For example, P. Wills of the Canadian Hydrographic Service reported that, "Effort by the Canadian Hydrographic Service to mine data from the IHO Data Center for Digital Bathymetry's (IHODCDB) crowd-source data for Notice of Mariner reports found approximately a half-dozen reliable reports in millions of data points", (Calder, 2018, Personal Communication). This demonstrates that although IHODCDB has compiled a large crowdsourced database of volunteered depth soundings, the probability that enough ships have measured the depth at a given location to reduce the sounding uncertainty to the point of qualification for hydrographic use, is vanishingly small. Although it is likely that data processing methods associated with identifying trusted portions of crowdsourced datasets will improve, it is highly probable that the current cost associated with extracting hydrographically significant data is prohibitively high.

A study was conducted to evaluate existing systems of collecting CSB, and to determine the viability of using crowdsourced data for hydrographic purposes (Hoy & Calder, 2019). This work confirmed that crowdsourced data is unable to meet charting standards at this time and is better relegated to ancillary tasks such as survey prioritization and change detection. However, a HO, such as NOAA's Office of Coast Survey, has a responsibility to notify mariners of potential hazards to navigation in a timely manner, and to publish new hazards in subsequent chart updates, even if the hazard is not reported by an authoritative source. In the United States, this is accomplished through the U.S Coast Guard's Local Notice to Mariners program, which provides a mechanism for any vessel to report a hazard for dissemination to the public.

In the case that a previously uncharted shoal is reported by a CSB source, it is standard practice for a HO to report the hazard, at least until the shoal can be verified by a trusted system. Hoy and Calder term this the "shoal-accepting method" in which the HO may publish a shoal reported by a non-authoritative CSB source because portraying this data serves only to, "Increase safety without introducing new risks" (Hoy & Calder, 2019, Section 7), even if the uncertainty associated with the data is unknown. The caveat to the shoal-accepting method is that CSB data should not supersede higher quality survey information in the case of navigationally significant waterways, where CSB reported shoals of dubious certainty may have major economic impacts (Hoy & Calder, 2019, Section 4). For most circumstances, there is a compelling ethical argument that a hydrographic agency has a duty to publish shoals from CSB systems even if the uncertainty associated with the soundings is unknown. However, this same lack of qualifying metadata makes CSB data largely impractical for any authoritative charting purpose, and a poor prospect as a hydrographic force multiplier (Hoy & Calder, 2019, Section 5).

In 2022, The Nippon Foundation GEBCO Seabed 2030 Project, which aims to collate all available data to produce a definitive map of global bathymetry by the 2030, estimated that 23.4% of world's seafloor has been mapped by echosounders (GEBCO, 2022). Despite major advancements in modern underwater survey technology, acoustically mapping the seafloor at high resolution is still an extremely time, resource, and financially intensive process. The contours of global seafloor maps are composed largely from satellite altimetry used to derive the rough shape of bathymetric features. The predicted bathymetry portrayed cannot be used for more than a general overview given the vertical uncertainty is on the order of 150 meters in the deep oceans, increasing to 180 meters between coastlines and the continental rise, and horizontal resolution on the order of 15 kilometers (Tozer et al., 2019). Therefore, both financial and scientific interest in understanding the true depth and shape of the seafloor continues to compound as people look for higher resolution bathymetric data sets not only for navigation, but as a fundamental data source to inform oceanographic models, climate models, fisheries management, infrastructure planning, etcetera.

To address the growing demand for higher resolution global bathymetry, The International Hydrographic Organization's (IHO) Data Centre for Digital Bathymetry (DCDB), which serves as the international hydrographic community's central repository for archiving and serving bathymetric data, announced they would begin accepting contributions of crowd sourced bathymetry (CSB) in 2020 (IHO, 2020). To combat some of the fundamental issues with collecting VGI from untrusted sources, as discussed above, the IHO has established a network of regionalized trusted nodes. A trusted node is defined as an organization or individual that serves as a data liaison between mariners collecting CSB data, and the DCDB. Each node serves the goal of providing localized services to improve the quality and uniformity of data collected by CSB vessels. They may assist their local CSB fleet with everything from sourcing data logging equipment, to providing technical support, to compiling the data and making sure it is properly formatted for delivery to the DCDB.

The Seabed 2030 initiative is an important contributor of VGI to the DCDB. This initiative was launched as a collaborative project between the Nippon Foundation of Japan and the General Bathymetric Chart of the Oceans (GEBCO), in 2017. It is an international effort to leverage existing and emerging technologies to collect new bathymetric data, and to collate all existing bathymetric data, with the goal of producing a definitive, publicly available, map of the world ocean floor at depth dependent resolution, by 2030 (Mayer et al. 2018). Efforts to collect quality CSB data for contribution to the DCDB are part of this initiative and are particularly essential data sources for remote regions.

Although these efforts demonstrate the international Hydrographic community's nascent efforts to develop acquisition and processing pipelines to utilize CSB data, there is still no way to guarantee the vast majority of CSB data can be trusted for hydrographic purposes.

# Prior Work

Through close collaboration with CCOM's industrial partner, SeaID Ltd., a data acquisition and processing system was developed to present an alternative to collecting unqualified data. It leverages a combination of cost-efficient hardware, paired with a vessel's existing echosounder to create a system for collecting, "Trusted Community Bathymetry" or TCB. A TCB system collects bathymetric data with quantified uncertainties in the horizontal and vertical directions, and therefore can provide the hydrographic agency a solution of known quality.

A TCB system's goal is to overcome the fundamental problems associated with collecting crowdsourced bathymetric data by moving away from a reactionary approach, and instead utilizing a combination of hardware and software that collects data qualified for hydrographic use by design. A TCB system is defined as one that can, "Provide data with sufficient guarantees that it can be used directly for hydrographic purposes, but at the same time be sufficiently simple that it can be installed unaided by the end user and run autonomously so that the user does not need to attend to it" (Calder et al., 2020).

Efforts to develop trusted systems beyond CCOM exist. The Hydroball and Hydrobox systems both present unique approaches to collecting trusted data (Rondeau et al.,2016, Rondeau, 2019). The Hydroball is an autonomous drifting or towed buoy equipped with a GNSS receiver, an inertial measurement unit, and a single beam echosounder. It is intended for surveying areas that are generally unreachable using classical survey launches (Rondeau et al., 2016). Alternatively, the Hydrobox is a small box that contains a GNSS receiver and an inclinometer. It must be connected to an existing echosounder on a host vessel to produce a georeferenced depth measurement. These systems present valid approaches to the problem but are tailored solutions to specific geographic areas and have cost or calibration requirements that make the technology hard to translate for scalable deployment worldwide.

The primary enabler for the development of the TCB system presented in Calder et al, 2020, is the availability of a low cost GNSS dual receiver with integrated motion sensor combined into a TCB system by CCOM's Industrial Partner, SeaID Ltd. With post-processing, this receiver can position its antenna to within a few centimeters in both the horizontal and vertical direction (Calder et al., 2020). SeaID Ltd. integrated this receiver with an Odroid C-2 embedded microprocessor, and a custom interface board to produce a functional TCB data logger. A Garmin GSD-25 echosounder with GT51M-TH transducer and NovAtel Pinwheel antenna were interfaced by CCOM to the SeaID data logger (SDL) to complete a prototype TCB system in fall, 2017. Three experiments, detailed in Calder et al., 2020, were conducted to assess the performance of the prototype system as follows:

1. **Static positioning over a U.S National Geodetic Service (NGS) horizontal control mark:** On 2017-10-31, a survey tripod was set up directly over an NGS horizontal control mark at Fort Point in New Castle, NH. Two, 3-hour, data sets were collected using both a Trimble Zephyr Geodetic antenna paired with a Trimble 5700 GNSS receiver, and a NovAtel Pinwheel antenna paired with the SeaID receiver. This experiment was meant to compare the SeaID receiver's ability to compute a precise and accurate 3D position solution to a survey grade system. With post processing, the SeaID receiver was able to resolve the antenna position with respect to the published control point with 0.02m error in the horizontal, and 0.043m in the vertical. Although its performance was unsurprisingly inferior to the survey grade system, the authors considered this performance to be adequate for resolving static positions in the TCB application.
2. **Static auto-calibration of vertical offset between the GNSS antenna and the transducer:** A NovAtel Pinwheel antenna and SeaID receiver were interfaced to R/V *Gulf Surveyor's* Garmin GSD-25 navigational echosounder, which broadcasts depth data via NMEA (National Marine Electronics Association) network packets. Recorded depths were compared to soundings from the ship's calibrated Odom CV200 survey-grade single beam echosounder. Both systems recorded data simultaneously for approximately 24 hours, while the boat sat dockside at a floating pier adjacent to a NOAA tide gauge. The experiment showed the TCB system is capable of statically calibrating the vertical offset between the antenna's phase center and the transducer as depicted in Figure 1. Most

importantly, this method resolved the known vertical offset value within the measurement's uncertainty envelope.

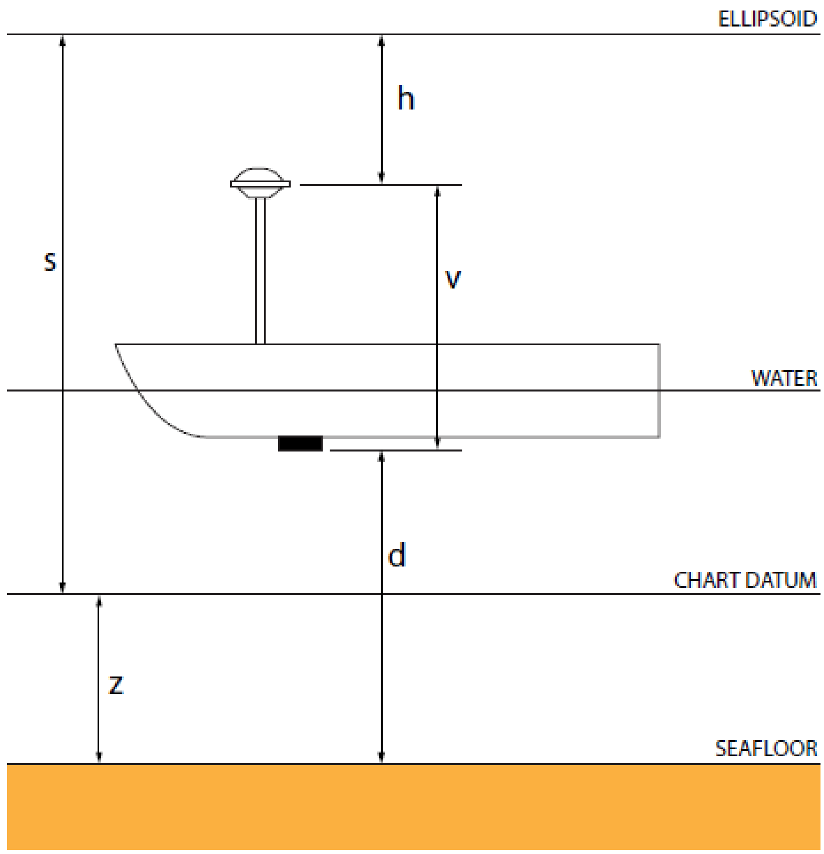


Figure 1: Configuration diagram for static calibration of the vertical offset, v, between the GNSS antenna phase center and echosounder, given knowledge of the depth to datum, z, and the datum-ellipsoid separation, s. Observed depth, d, and antenna height, h, are measured by the system (Calder et al., 2020). A NOAA tide gauge installed at the adjacent USCG pier measured the water level. (Station ID: 8423898) (Figure from Calder et al., 2020, with permission)

3. **Underway uncertainty and positioning calibration:** R/V *Gulf Surveyor's* configuration was the same as that was used for the auto-calibration experiment. While underway, she completed a series of maneuvers, and transited a section of the Piscataqua River. Depth uncertainties were evaluated in varying water depths, magnitudes of vessel motion, and near overhead structures that may pose multipath degradation of the GNSS solution. The

composite latency of the Garmin-SeaID pair was estimated as 1.585s using a nested grid-search of the cross-correlation between the zero-mean versions of the signals since the depths lag the observed height variations, and the effects of speed and motion on depth uncertainty were effectively captured by the GNSS antenna (See Figure 2). Most significantly, the experiment showed that outside of strong multipath environments, and in the depth regimes considered (14-15 m below datum), the prototype TCB system can achieve Total Vertical Uncertainty (TVU) within the IHO's Order 1b survey requirements (Calder et. al, 2020); (IHO Standards for Hydrographic Surveys, 5th Edition, 2008) .

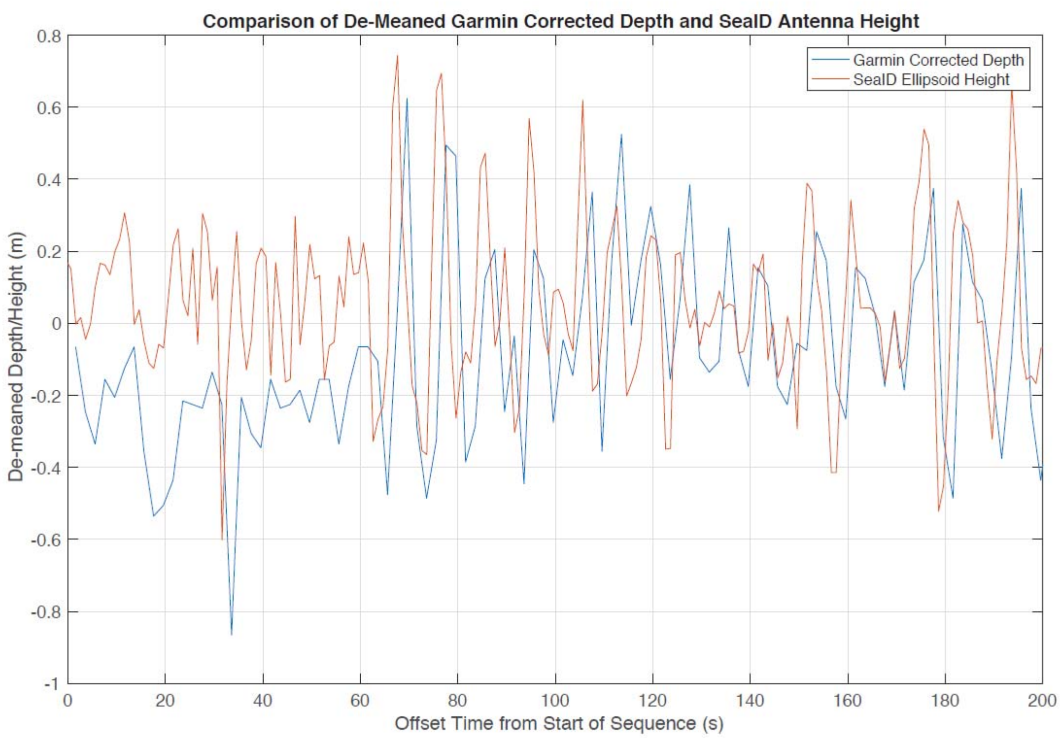


Figure 2: Comparison of Garmin observed depths and SeaID data logger (SDL) antenna heights, demonstrating that the motion effects are captured in the antenna height to some extent as well as in the depths, and that there is a significant latency in the timestamps associated with the Garmin observations logged by the SDL. Note that the means have been removed from both signals to allow for plotting on the same scale (Figure from Calder et al., 2020, with permission).

The results of these experiments suggest that the prototype TCB system can meet the horizontal and vertical positioning requirements required to qualify the data for some level of hydrographic use. However, there are still several improvements worthy of consideration.

One recent improvement is the development of methods to automate estimation of the horizontal offset between the antenna and transducer using practical alternatives to land surveying methods (O'Heran & Calder, 2021). Compensation for this offset is valuable in minimizing horizontal sounding uncertainty, which can be especially significant on large vessels, and especially problematic in narrow channels or waterways. In this work the authors present promising methods for horizontal offset calibration using either LIDAR or photogrammetric data acquired by an unmanned aerial vehicle with centimeter-level horizontal deviation estimates. In practice, this technology provides an efficient, unobtrusive, and inexpensive way to quantify horizontal sounding uncertainty on TCB vessels without requiring the operator to dry dock or be responsible for any sort of measurement procedure.

## Motivation

Three major advancements to the TCB system design motivated the work contained in this thesis:

**Significant reduction in total system cost:**

Although the prototype TCB system presented in Calder et al., 2020 is remarkably inexpensive (~$2000) in relation to its capability, its cost is still prohibitive to mass production and widespread distribution amongst vessels of opportunity. The most expensive component in the prototype system is the survey-grade NovAtel antenna, which retails for ~$1000. However, the real-time precision the NovAtel antenna provides is not critical for a TCB application. TCB data is meant to be collected in the background, without disrupting a vessel's normal activities, and then offloaded to a central repository when appropriate. There is no need for real-time data products. Since the TCB datalogger is capable of recording the raw GNSS observables in a compact format that can be exported in the Receiver Independent Exchange Format (RINEX) using custom code provided by SeaID, it is possible to record lower quality observations using a less expensive antenna, and then to reduce the magnitude of the errors in the recorded positions via post processing the data by establishing a baseline to a local NOAA CORS[1] station.

This thesis establishes the Harxon GPS500 antenna as a stable, cost-effective, alternative to the NovAtel antenna and demonstrates a post-processing workflow that provides final position solutions well within the uncertainty budget for hydrographic use.

This work is addressed in Chapter 1: Evaluating the Harxon GPS500 Antenna.

**Adding sidescan capability to a TCB system:**

The TCB system prototype presented in Calder et al., 2020 interfaces with a vessel's existing single beam echosounder, using a common NMEA[2] depth sentence for depth information to facilitate compatibility with as many vessel configurations as possible. Single beam echosounder geometry inherently requires the TCB equipped vessel to pass over a target of interest to verify its presence, which is especially problematic if the target is a potential hazard to navigation. Furthermore, single beam soundings simply provide a depth at a point along a vessel's track line and require many passes to accumulate enough point density to, say, resolve the shape of a bathymetric feature.

Alternatively, many modern recreational echosounders, including the Garmin transducer used for the TCB demonstration, include a high frequency sidescan imaging array integrated into the

[1] CORS- Continuously Operating Reference Station: https://geodesy.noaa.gov/CORS/
[2] NMEA- National Marine Electronics Association

transducer housing. Sidescan sonars create a two-dimensional image of the seafloor by transmitting a fan shaped pulse to ensonify a wide swath of seafloor perpendicular to the path of the transducer. The total width of the ensonified swath is usually equivalent to several times the water depth in a given area. This imagery can be used to detect changes in bathymetric features by comparing the presence or absence of acoustic targets at various epochs, and by comparing the acoustic shadows cast by ensonified targets to reveal features of the target's shape. It can also be used to discern the relative echo strength of targets, which can be interpreted as an indicator of the target's density, hardness, or aspect. Finally, sidescan systems are capable of imaging water column targets such as fish or the mast of a wreck. Perhaps most important for the TCB application, a sidescan sonar can be used to facilitate stand-off observation of a suspected obstruction, without requiring a TCB vessel to approach a potentially chartable danger.

This work is addressed in Chapter 2: Reverse Engineering the Garmin GCV-10 Side Scan Module, and Chapter 3: Integrating the Garmin GCV-10 with a TCB Datalogger.

**Demonstrate an operational model for autonomously collecting sidescan imagery from a TCB vessel:**

This thesis develops and demonstrates an operational model in which a TCB datalogger may integrate with a vessel's existing sidescan sonar and provide capacity to autonomously control and collect imagery from the unit with no input from the vessel crew. In this model, a HO may upload a series of waypoints for hydrographic areas of interest to a TCB datalogger. Then, as the vessel goes about its normal activities, the system will detect when the ship is within sidescan range of a waypoint, turn on or start recording the imaging data, and turn off or stop recording the sensor when the vessel exits the area. It is also possible for the HO to include specific sidescan settings (range, frequency, time varying gain, etc.) that will automatically be applied during data collection in a particular area.

This work is addressed in Chapter 3, Section 3.5: Autonomously Imaging Sidescan Targets in the Field.

## Contribution

This thesis presents a major hardware cost reduction made possible by demonstrating that with post-processing, the Harxon GPS500 antenna can provide position uncertainties on the same order as the survey grade NovAtel antenna used in the original prototype, for approximately one-fifth of the cost. This development represents a very substantial (40%), reduction in total system cost, and makes the TCB package significantly more suitable for mass production. Notably, the system automatically provides geodetic positioning in the WGS84 reference frame making it easily integrated with other ocean mapping datasets.

The other major contribution of this work is the substantial advancement in TCB system capability presented by the integration of a low-cost recreational sidescan module, which can be operated autonomously by the TCB datalogger with no user input. This represents, to our knowledge, the first recreational sidescan integration into a third-party system which provides access to raw imagery, the ability to georeference the imagery with known uncertainties in the vertical and horizontal, and data compatibility with standard hydrographic software packages for post-processing. Furthermore, we demonstrate a concept for operations in which the Garmin GCV-10 can be operated autonomously using the TCB datalogger's embedded computer for both command/control and data storage.

The availability of high-resolution sidescan imagery adds significant richness to the dataset a TCB vessel can collect by producing a two-dimensional swath of sonar coverage that extends far abreast of the vessel track line. This imagery provides the HO a much broader ‘field of view’ to detect shifting bathymetry, hazardous objects, or water column targets.

Beyond the HO, the availability of a high-resolution, low-cost, sidescan survey package capable of producing precise geodetic-referenced imagery, has greater implications in habitat mapping, water-column mapping, geological mapping, fisheries science, search, and recovery, or in producing inexpensive and lightweight packages for outfitting unmanned vessels such as ASV’s or ROV’s.

# CHAPTER 1: EVALUATING THE HARXON GPS500 ANTENNA

## 1.1 Introduction

To address the uncertainty problems associated with CSB systems, the prototype TCB datalogger presented in Calder et al., 2020, utilizes an integrated GNSS receiver developed at University of Texas at Austin, and licensed to CCOM industrial partner SeaID Ltd., to provide high precision, high accuracy, geodetic referenced 3D position solutions, and the ability to autonomously calibrate the vertical installation offset between a vessel's GNSS antenna and echosounder transducer. The combination of these capabilities eliminates two major barriers to a hydrographic organization's ability to utilize this data for charting purposes: 1) The need for a "crowd", since the GNSS data can be post-processed and integrated with echosounder data to produce soundings with quantified uncertainties in the vertical and horizontal. 2) Dependence on the end user to ensure data quality since the system can calibrate itself in the vertical direction and collect data autonomously.

For reference, the prototype TCB datalogger, presented in Calder et al. 2020, was capable of exceeding IHO S.44[12] Order 1b[3] total vertical uncertainty requirements in the depth regime considered (14-15m below datum). These results demonstrated the TCB system can collect hydrographically viable data, although the total cost (~$2000) for this prototype is potentially prohibitive to widespread implementation.

To substantially reduce the hardware cost for a TCB system the Harxon GPS500 is considered here as a low-cost alternative to the NovAtel Pinwheel antenna. The Harxon GPS500 retails at an order of magnitude lower price (~ $200) than traditional marine survey GNSS antennas

[3] IHO S.44 [12] Order 1b requires a TVU of no more than 0.53-0.54m (95%)

and receives GPS L1/L2, GLONASS L1/L2 and BeiDou B1/B2/B3 signals. Here we detail a 10-day experiment to evaluate the precision, accuracy, and performance stability of the Harxon GPS500 antenna and its suitability for use in a TCB system.

## 1.2 Methods

The Harxon GPS500 mini survey antenna[4] was mounted to a fixed antenna mast, with an unobstructed sky view, on the roof of the Center for Coastal and Ocean Mapping (CCOM) at the University of New Hampshire (UNH) (Figure 3). The antenna was connected to the SeaID receiver with an impedance matched ultra-low loss coaxial cable[5] and data was continuously logged for ten days (2018-08-03 – 2018-08-12) to evaluate performance throughout cyclic variations in the ionosphere.

[4] Antenna serial C17100000990
[5] SLA, INC. cable model CXTG247G-15M. 50Ω impedance.

Figure 3: Harxon GPS500 antenna mounted on the rooftop of the CCOM wing of the Chase Ocean Engineering building.

Each day, raw GNSS observation data were converted from the logger's binary format to Receiver Independent Exchange (RINEX) file format using code provided by SeaID. RINEX files were post-processed using RTKLIB[6], an open-source package for GNSS positioning (Takasu, 2009). A position solution was computed for each epoch in addition to a single point solution for all epochs in each 24-hour observation period. The positioning uncertainty was reduced by double differencing the GNSS observations using data from a nearby Continuously Operating Reference Station (CORS)[7], managed by the National Geodetic Survey (NGS) (Figure 4). The code, plotsinglesolutions[8], was used to translate the single point solutions from geodetic (WGS84)

[6] rtklib.com
[7] Station ID: NHUN. Baseline distance: 1277m
[8] Appendix A: Table of Software

coordinates to Earth Centered Earth Fixed (ECEF) Cartesian coordinates to calculate the baseline distance to the CORS, and the three-dimensional dispersion of single point position solutions. The code was also used for a final translation to topocentric East-North-Up (ENU) coordinates to align the XY axis to the local horizon plane. The averaged location of the antenna for the entire set of observations was used as the origin for the local ENU coordinate system.


Figure 4: Satellite imagery showing relative locations of NOAA CORS Station (NHUN) and the Jere A. Chase Ocean Engineering Laboratory (highlighted in yellow), where the experiment took place. The baseline distance between the two antenna locations is 1277m. Image taken from NOAA CORS Map online: https://geodesy.noaa.gov/CORS_Map/.

Additionally, the same 24-hour subsets of observations were downloaded and submitted to the U.S. NGS Online Positioning User Service (OPUS), to confirm the stability of the RTKLIB processing and to confirm the positioning solution's precision with reference to three local CORS control points. The antenna reference point height was entered into OPUS as '0' so position solutions would be reported with respect to the antenna's phase center for consistency with RTKLIB results.

## 1.3 Results

Post-processed position solutions using RTKLIB to address all epochs during each of the ten days of observations showed that the Harxon GPS500 antenna and SeaID receiver are capable of stable, high quality, observations. Figure 5 demonstrates the tight distribution of solutions at all epochs for one 24-hour observation period. Figures 6 & 7 show the geographic distribution of single point solutions computed as a single best estimate of position from all epochs observed during a single day. These figures demonstrate that, with post-processing, the TCB prototype was able resolve the three-dimensional position of the antenna's phase center to a standard deviation of one centimeter on each axis throughout the experiment's duration.

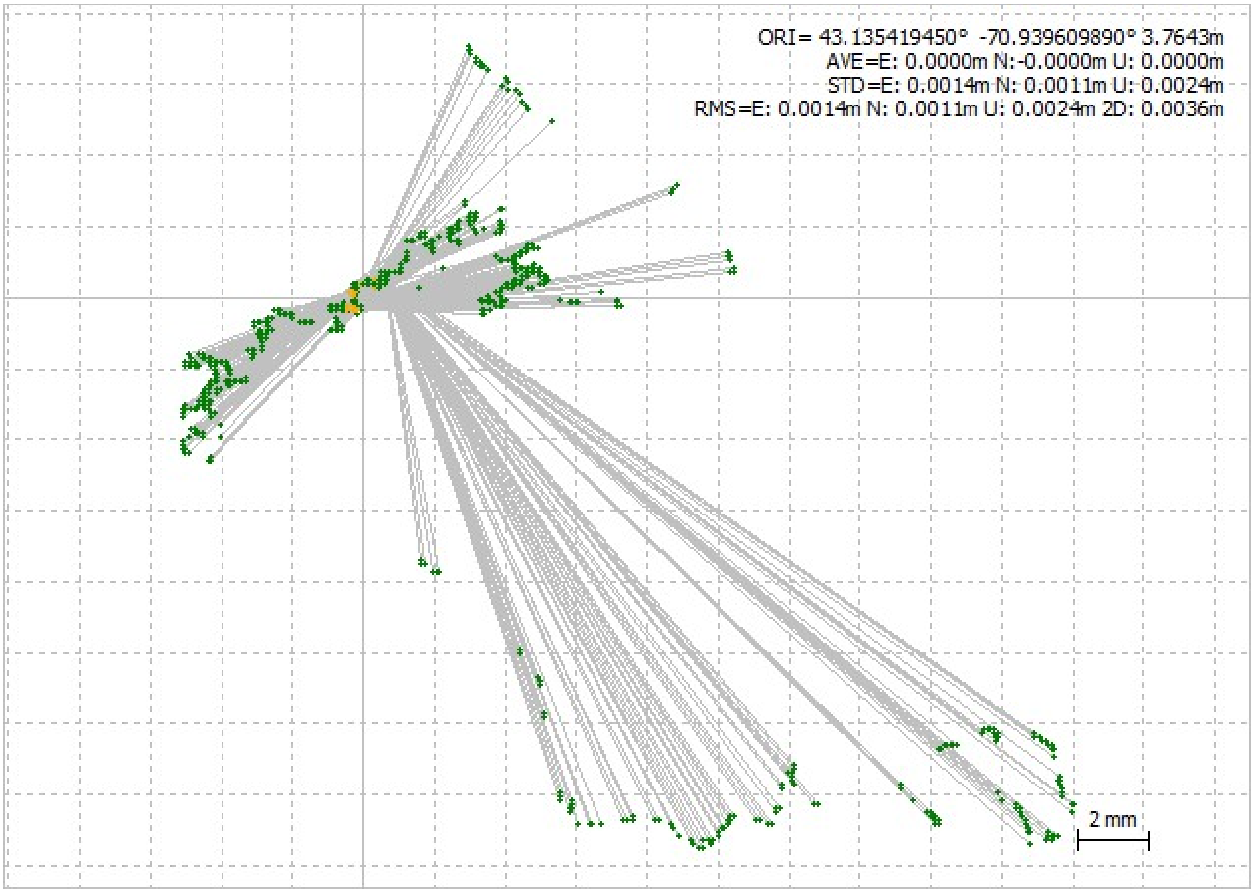


Figure 5: Geographic distribution of post-processed positioning solutions using RTKLIB from 2018-08-09 00:00:00 GPST through 2018-08-09 23:59:59 GPST. Green are fixed ambiguity solutions, yellow are floating point solutions.

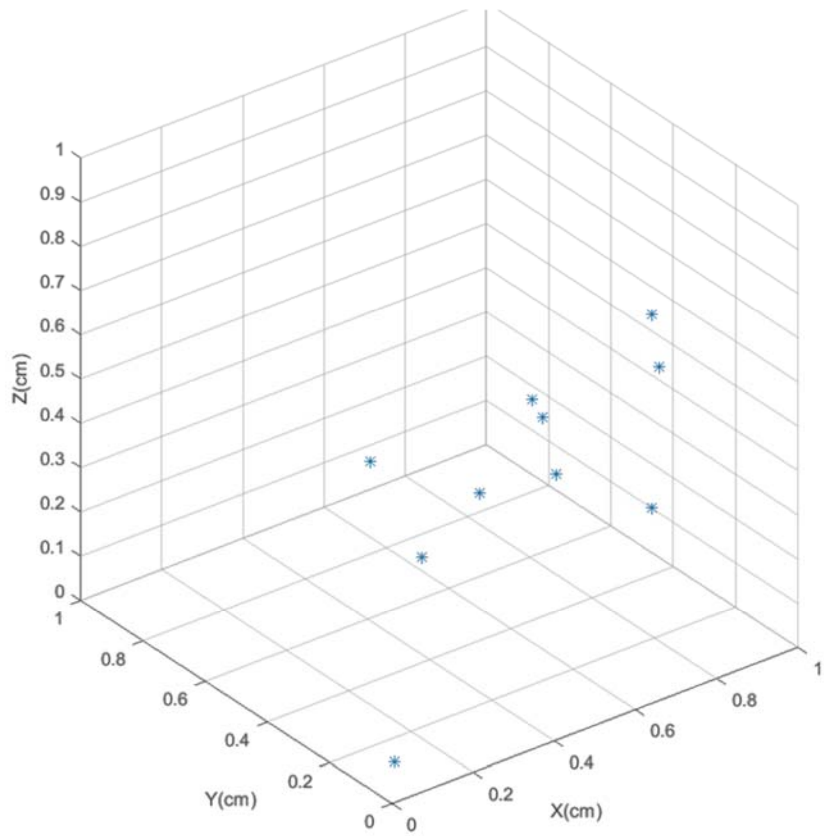


Figure 6: Single point (24hr) position solutions from the Harxon GPS500 antenna and SeaID receiver displayed in Earth Centered Earth Fixed (ECEF) Cartesian coordinate system with the mean position removed from each axis for simplicity of interpretation.

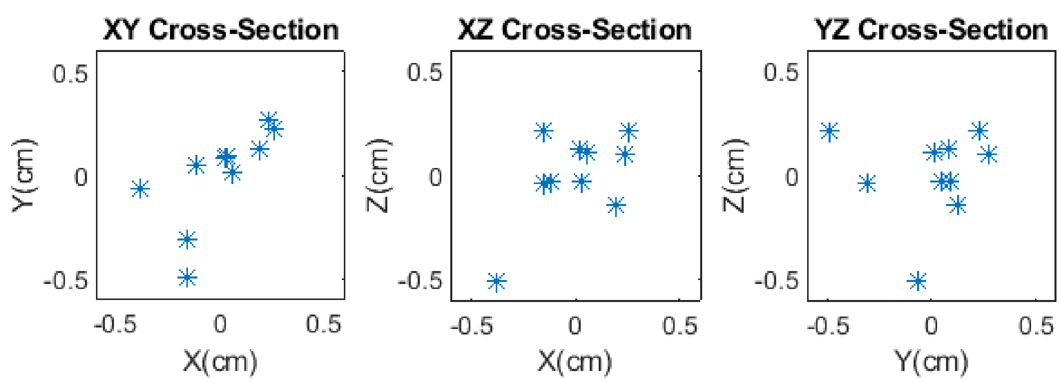


Figure 7: : Two-dimensional cross sections of 10 single point (≈24hr) position solutions from the Harxon GPS500 antenna and SeaID receiver presented in East-North-Up (ENU) Cartesian coordinate system, whereas the East-North (XY) plane is the local horizon plane, and the origin is the average estimated location of the antenna for the entire set of observations. The mean was removed from each axis for simplicity of interpretation.

The magnitude of daily errors reported by OPUS were consistent with RTKLIB derived results, Table 1. Position uncertainty was on the order of 1-5cm for the experiment's duration.

Table 1: Peak-to-peak position error reported by OPUS for solutions with three different CORS stations.

| **Date** | **Lat. Peak Error (cm)** | **Lon. Peak Error (cm)** | **Hgt. Peak Error (cm)** |
|---|---|---|---|
| 8/3/2018 | 1.1 | 0.9 | 0.8 |
| 8/4/2018 | 1.1 | 0.9 | 3.2 |
| 8/5/2018 | 1.1 | 0.9 | 4.6 |
| 8/6/2018 | 0.6 | 1.1 | 3.4 |
| 8/7/2018 | 2 | 0.6 | 0.5 |
| 8/8/2018 | 1.9 | 0.6 | 0.8 |
| 8/9/2018 | 0.1 | 0.2 | 1 |
| 8/10/2018 | 1.6 | 0.9 | 1.7 |
| 8/11/2018 | 2.5 | 0.6 | 4.7 |
| 8/12/2018 | 0.5 | 1 | 1.2 |
| | | | |
| **Max Peak Error** | 2.5 | 1.1 | 4.7 |
| **Mean Peak Error** | 1.25 | 0.77 | 2.19 |

The code, plotsinglesolutions, was extended to compare the baseline distance from the Harxon antenna to the NHUN CORS base station reported by OPUS to the baseline distance calculated using the RTKLIB derived single point solution for each day of the experiment. The baseline distance from each RTKLIB single point solution to NHUN was calculated using Pythagoras' theorem, since the distance is short enough that a geodetic solution is not required. The peak discrepancy between processing methods was 4cm, with calculated baselines of 1277.0m and 1276.96m for OPUS and RTKLIB respectively.

## 1.4 Discussion

This experiment demonstrates the Harxon GPS500 antenna can make consistent, high-quality observations that provide uncertainties well less than a decimeter on each axis, with post-processing. This level of uncertainty is on the same order as results from the survey-grade antenna used in the static calibration experiment in Calder et al., 2020, and is well within the error budget for a TCB application. The vertical peak-to-peak error of 4.7cm is nearly identical to the 4.3cm peak error recorded from the Novatel Pinwheel antenna and SeaID receiver combination tested in Calder et al., 2020, and is particularly promising due to the more stringent constraint on vertical uncertainty in a TCB application.

Comparison of RTKLIB and OPUS reported peak-to-peak error and baseline calculations to a known control point proved the stability of RTKLIB and validated its use in reliably post-processing GNSS observations from the Harxon GPS500 and SeaID receiver combination.

## 1.5 Conclusion

The Harxon GPS500 antenna is a reliable and cost-effective alternative solution to a traditional survey antenna for the TCB application. With post processing, the system could provide observations with uncertainty on the same order as those from the NovAtel survey antenna used for the prototype presented in Calder et al., 2020. Throughout the 10-day test period the Harxon GPS500 collected observations with horizontal peak error <3cm, and vertical peak error <5cm, when kinematic positioning was achieved using rapid GNSS satellite ephemeris data.

# CHAPTER 2: REVERSE ENGINEERING THE GARMIN GCV-10 SIDE SCAN MODULE

## 2.1 Introduction

The TCB system design presented in Calder et al., 2020, can utilize echosounder data transmitted on a host vessel's NMEA[9] network. Since NMEA communication protocols are highly standardized and nearly ubiquitously implemented in marine navigation electronics equipment, the TCB system can collect depth data from the widest possible variety of echosounders by logging the NMEA "depth below transducer" (DBT) datagram. While this data is valuable, its utility is limited in that it only provides single-point depth values along the vessel's track line.

Alternatively, many modern recreational sonars now include high-frequency side-scan modules capable of producing a high-resolution acoustic image of the seafloor along the direction of travel. Since the swath of side scan sonar coverage grows proportionately with water depth, and can extend far abreast the vessel's centerline, integrating this technology allows a TCB equipped vessel to record a stand-off acoustic image of a target as it passes by at a safe distance.

As a result of the vastly increased data volumes associated with producing high-resolution side-scan imagery, modern sonars communicate using an Ethernet-based network protocol, proprietary to the manufacturer, in lieu of traditional NMEA datagrams. Prior to undertaking this research, a thorough audit of existing side-scan sonar modules suitable for integration with a TCB system was conducted, and it was found that no published network protocol exists for interacting with a commercially available unit. Therefore, one of them was chosen for reverse engineering to

[9] NMEA- National Marine Electronics Association.

establish compatibility with the prototype TCB system. No data protection scheme was detected during this work.

The Garmin GCV-10 was chosen due to its competitive price, technical specifications, and market availability at the time this work began. It is sold for approximately $500 with a GT30-TM transducer included to add scanning echosounder functionality to a compatible Garmin chart plotter. It can produce high-resolution single beam and sidescan imagery with frequency modulated (CHIRP) pulses centered at 455 kHz (425-485 kHz) and 800 kHz (790-850 kHz) and includes a temperature sensor integrated into the transducer housing. The sidescan beam width is 1.1° along x 53° across track at 455 kHz or 0.7° along x 30° across track at 800 kHz, which is narrow compared to competitive units. The unit is tolerant of 10-35VDC power input and draws 10.5W maximum.

A field test was conducted to determine that raw side-scan data is logged at a maximum rate of 12 megabytes per minute in very shallow water and decreases to 3 megabytes per minute in very deep water (See Appendix A: Data Volume Experiment). Therefore, the TCB datalogger may log between 22 and 88 hours of continuous sidescan data before filling a $16, 128GB SD card[10]. When the card is full the data can be downloaded, and the card reused. This work showed that logging sidescan imagery required no significant hardware change or cost addition to the existing TCB system design.

## 2.2 Structure of a Garmin Installation

A standard Garmin GCV-10 installation provides for echosounder display and control via a compatible Garmin multifunction display (MFD), Figure 8. The MFD connects to the GCV-10

[10] Based on SD card pricing in early 2022.

processor using a standard Ethernet cable, and up to three MFD's can be connected to the 3-port Ethernet hub built into the processor enclosure. The GCV-10 processor has an independent DC power supply which provides power to the transducer.

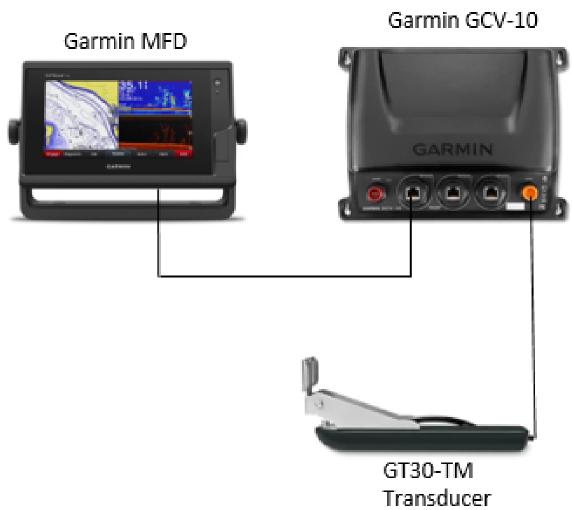


Figure 8: Generic Garmin GCV-10 installation schematic.

## 2.3 Methods for Network Protocol Analysis

To reverse engineer the network protocol the Garmin GCV-10 uses to communicate with a compatible MFD, a passive Ethernet tap[11] was inserted between the GCV-10 processor and Garmin 742XS chart plotter (Figure 9). This device consists of four Ethernet ports which are wired so that two ports support bi-directional LAN traffic (pass-through ports), and two ports are receive-only (monitoring ports). The two pass-through ports were used to connect the echosounder processor and chart plotter, while a laptop running Wireshark[12] network traffic capture software,

---

[11] The Throwing Star LAN Tap was used for this project. More information can be found here: https://greatscottgadgets.com/throwingstar/

[12] Wireshark is a free and open-source network packet analysis program. Project website http://wireshark.org/

was connected to one of the two receive-only monitoring ports. The passive nature of this tap makes it undetectable to devices connected to the pass-through ports, while the network capture laptop can be connected to each of the two monitoring ports to capture traffic moving in a single direction.[13]

Initial network analysis was conducted with the transducer submerged in a bucket of room temperature tap water to minimize variation in the sensor's environment and reduce the network traffic complexity.


Figure 9: Wiring schematic for passively sniffing network traffic between the echosounder processor and chart plotter using a Throwing Star LAN Tap and a laptop running Wireshark.

Network traffic analysis revealed that eleven multicast groups and one TCP/IP connection are automatically configured between the GCV-10 processor and chart plotter during startup. It was found that the single TCP/IP connection facilitates the command-and-control connection

[13] Note that an unmanaged switch with a mirrored port was tested as an alternative to a passive tap and caused total loss of communication between Garmin devices. A technical explanation for this is beyond the scope of this paper but an IGMP unaware switch may be suitable for packet sniffing.

between the sonar processor and chart plotter. We will refer to this connection as the **Control Data Stream**. Additionally, one multicast group is used to send digitized sidescan sonar imagery from the processor to the chart plotter. We will refer to this connection as the **Image Data Stream**. The other multicast groups were determined to be irrelevant for the purposes of this research and were not investigated further. It is likely these groups are configured to exchange and synchronize data with compatible Garmin network services or devices not used in this research.

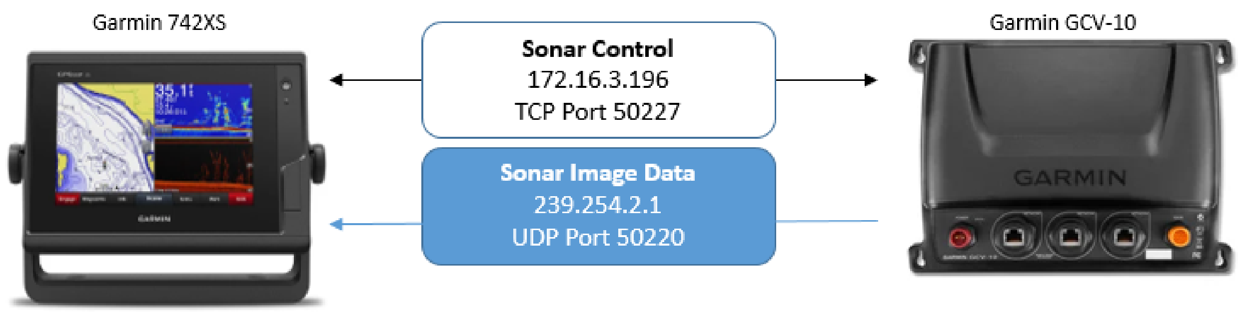


Figure 10: The Control and Image Data streams. Commands for echosounder control are sent to the GCV-10 processor at static IP address 172.16.3.196 on port 50227. The echosounder image data is broadcasted on UDP multicast address 239.254.2.1 to port 50220.

## 2.4 Control Data Stream

The **Control Data Stream** was identified by using a LAN tap and Wireshark to analyze network packets traveling from the chart plotter to the GCV-10 processor while the echosounder was not transmitting. By establishing an understanding of the network traffic in this 'steady state', and then changing echosounder settings (i.e., range, frequency, gain, etc.) using the chart plotter, it was possible to correlate changes in network traffic to application of echosounder settings.

Once it was determined that all commands are transmitted on the same TCP/IP connection, the datagrams containing commands associated with each echosounder control setting could be identified. To do this, a single echosounder setting was toggled while Wireshark captured traffic to the GCV-10 processor and filtered out the **Control Data Stream.** In this method, built-in Wireshark functionality could be used to correlate a specific network packet to a time an echosounder setting was applied, to remove the TCP header, and to extract the data payload containing the command string. This method was used to determine the command datagrams to modify the echosounder settings in Table 2.

Table 2: Reverse engineered controls for Garmin GCV-10.

| **Setting** | **Option** |
|---|---|
| System Power | On/Off |
| Transmit | On/Off |
| Frequency | 455kHz/800kHz |
| Interference Filter | High/Medium/Low/Off |
| Range | User Defined/Auto |
| Time Varying Gain | High/Med/Low/Off |

To implement this functionality, custom Python code was written to transmit sonar control commands directly from the TCB Datalogger's integrated Odroid C2 computer to a network port on the GCV-10 processor[14].

[14] See Appendix A: Table of Software: GCV-10 Commands

## 2.5 Image Data Stream

The **Image Data Stream** is transmitted from the GCV-10 processor's network ports in the form of multicast UDP datagrams. This data stream was identified by using a LAN tap and Wireshark to compare conversation traffic volume when the GCV-10 is transmitting versus secured. The GCV-10 fragments each full sidescan scanline into 14 UDP datagrams, which are sent in sequential groups of seven, alternating between port and starboard data payloads. Individual datagram payloads were converted from binary to hexadecimal values for parsing, and then to 8-bit unsigned integers to reproduce sidescan imagery. Each datagram carries data blocks to produce three distinct visualizations of the digitized scanline. For simplicity, these visualizations will be referred to as Viz 1, Viz 2, and Viz 3. Figure 11 shows the basic structure of a datagram containing sidescan imagery in the **Image Data Stream**.


Figure 11: Basic imagery datagram structure consists of a variable length Ethernet header and data payload header followed by a variable length header to precede the standard-length data payload for each visualization.

Since **Image Data Stream** datagrams incorporate multiple variable length headers it was necessary to reverse engineer patterns in the datagram payloads. This enables parsing out sidescan data programmatically. The following rules were developed for parsing[15]:

[15] A link to a programmatic application of these rules is provided in Appendix A: Table of Software: PARSER_basic.m

1. Byte #5 of the Data Header encodes the total number of bytes in the datagram payload in hexadecimal format. Convert the hexadecimal number to an 8-bit unsigned integer and then add 1032 to find the payload size.

   Example: $B_5 = 0xDF = 223_{10}$
   223 + 1032 = 1255 bytes

2. Byte # 13 of the Data Header encodes which side of the transducer the datagram should be associated with, port or starboard.

   Port = 00 or 03
   Starboard = 01 or 02

3. Each Viz header is terminated with a four-byte sequence determined by payload length.

   a. If the datagram payload length is between 1000-1100 or 1200-1300 bytes, the last four bytes of the Viz header is:
      Viz 1 - [DA 04 D8 04]
      Viz 2 & 3 - [AE 02 AC 02]

Three distinct visualizations of the sidescan record can be reassembled from the datagrams (Figure 12). Viz 1 is likely the raw digitized sidescan data due to the relatively small dynamic range in pixel values and 8000-pixel swath width. Viz 2 and 3 are two-byte averaged versions of Viz 1 with a total swath width of 4000 pixels. Viz 2 is dynamic range adjusted to emphasize the highest impedance contrasts in the image. Viz 3 is the product of averaging every two pixels in Viz 1 to stretch the total dynamic range of the dataset and produce a higher contrast image (Figure 13). The Garmin 742XS chart plotter displays sidescan data in the Viz 3 format, therefore, the remainder of this thesis uses the Viz 3 format as the demonstrator.

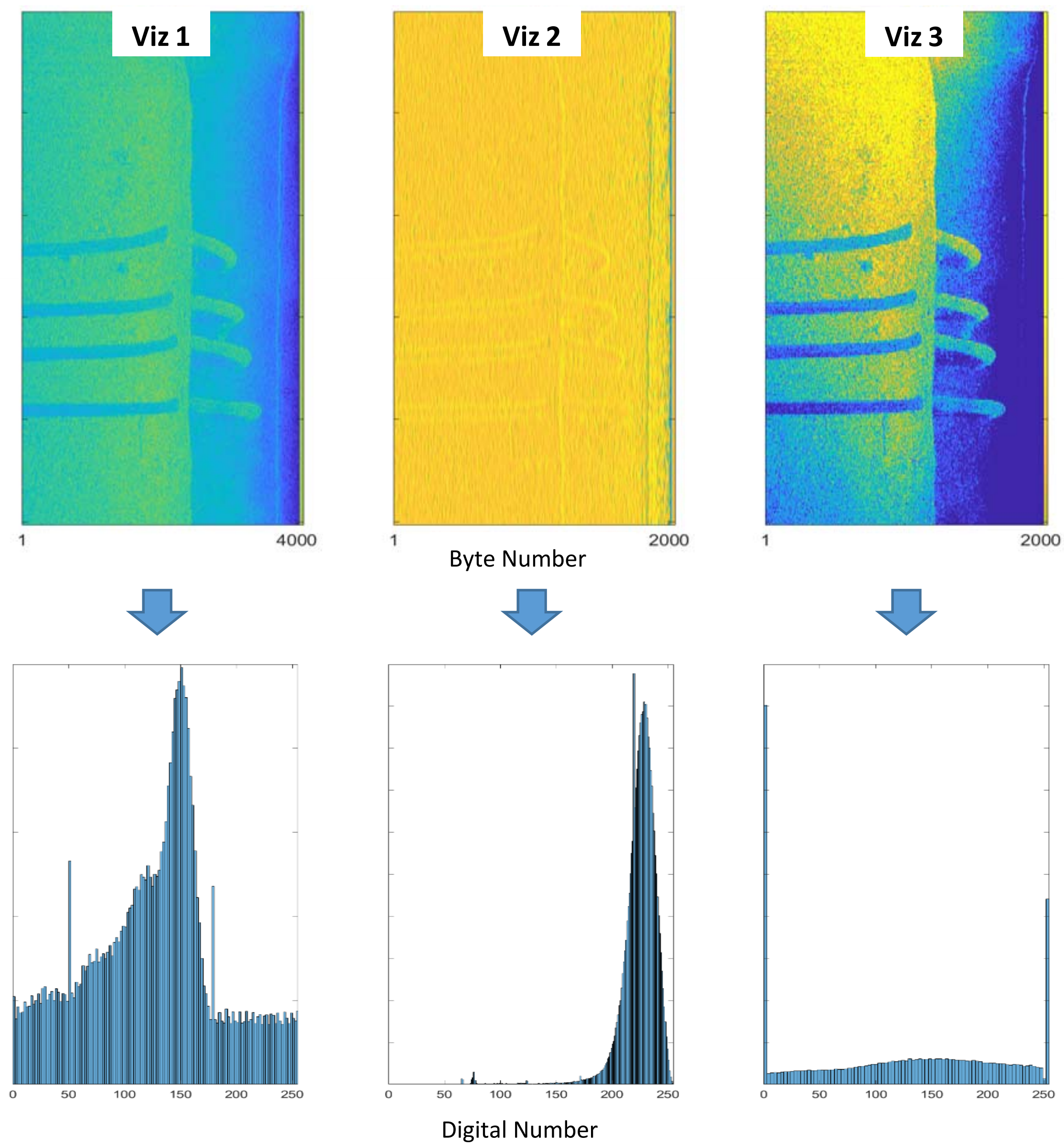


Figure 12: Three visualizations of the same portside sidescan record of four bridge pilings produced by the Garmin GCV-10 (Top) and their corresponding histogram (Bottom).

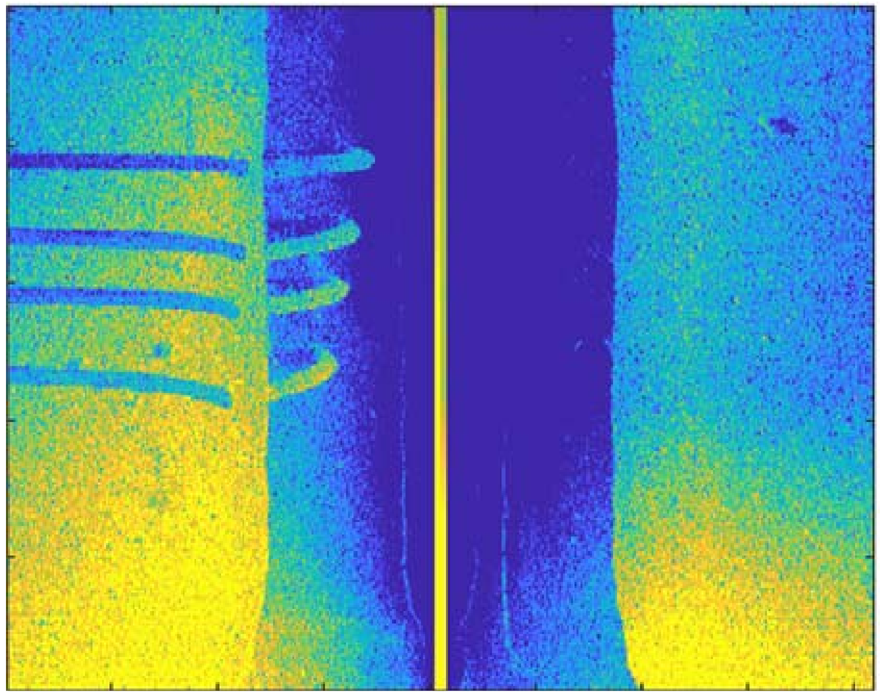

Figure 13: Viz 3 records of full sidescan swath reconstructed using custom MATLAB code. One scanline is composed of 4000 pixels.

## 2.6 Conversion to XTF Format

Code to reassemble the sidescan record from the **Image Data Stream** was extended to convert the data into "hydrographically friendly" XTF[16] format, allowing it to be handled through standard software packages for hydrographic data, Figure 14. The XTF converter code is a custom adaptation of the open source "pyxtf" Python library[17] and is called xtf_converter_TCB.

The XTF converter code integrates the navigation data with the sidescan imagery to produce a georeferenced XTF file. In addition, the code automatically enters the sidescan channel

[16] Extended Triton Format (XTF) Rev. 26 documentation: https://www3.mbari.org/products/mbsystem/formatdoc/XtfFileFormat_X26.pdf
[17] pyxtf Github Repository: https://github.com/oysstu/pyxtf

number, beamwidth, frequency, and the slant range associated with each scanline in the XTF file metadata.

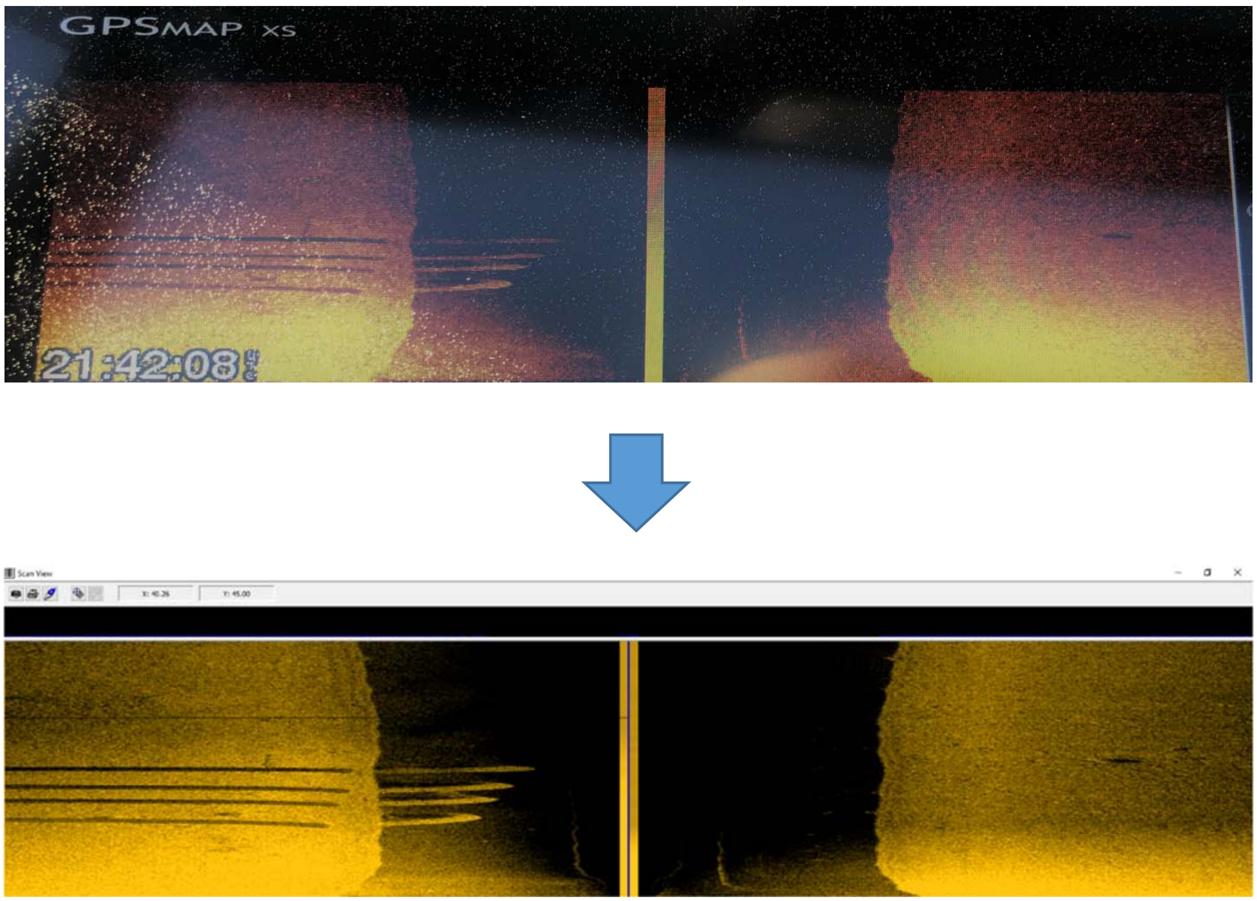


Figure 14: Photo of real-time sidescan imagery displayed on Garmin GPSMAP 742XS chart plotter (Top). Reconstructed Garmin GCV-10 sidescan imagery converted to XTF format using the XTF Converter code and rendered with the Hypack[18] Targeting and Mosaicking utility.

[18] Hypack is a common hydrographic industry software package: https://www.hypack.com/

# CHAPTER 3: INTEGRATING THE GARMIN GCV-10 WITH A TCB DATALOGGER

## 3.1 Introduction

This chapter leverages the code developed in previous sections to demonstrate a method for using a TCB Datalogger to control the Garmin GCV-10 and to log sidescan imagery from the **Image Data Stream**. The code, xtf_converter_TCB, was developed to integrate the sidescan imagery and post-processed position observations to produce a georeferenced sidescan record in hydrographically friendly, XTF file format. To improve the positioning precision of the integrated data, a desktop experiment followed by a field verification was conducted to quantify and compensate for the latency between the sidescan and navigation information.


Figure 15: Physical installation schematic for logging sidescan data using the SeaID prototype TCB datalogger. The Garmin MFD is optional because the echosounder can be controlled solely with the TCB Datalogger if there is no need for a real-time data display.

## 3.2 Logging Side Scan Data with the TCB Datalogger

The TCB datalogger was connected to an open network port on the Garmin GCV-10 with a Cat6 ethernet cable. Tshark[19] -- a lightweight (~300kB) network packet capture and analysis program that runs under a command line interface was installed on the TCB datalogger. This program includes a network traffic dump tool called Dumpcap[20], which allows the user to filter and capture data from a live network and write the packets to file. Dumpcap was used to filter UDP datagrams containing sidescan imagery from the **Image Data Stream** and store the capture files on the datalogger's SD card in next-generation packet capture file format, PCAPNG (Tuexen et al., 2021). This is a binary file format with support for nanosecond-precision timestamps.

This method of logging sidescan data is advantageous because it requires very little computing power and eliminates extraneous network traffic from being logged to the device's SD card. The Odroid embedded computer, like all low-cost embedded systems, has limited capabilities, and therefore the data processing and storage efficiency demonstrated in this method is advantageous for keeping hardware costs low. When sidescan data is logged in shallow water, generating data rates up to 12MB/minute[21], the Linux process manager shows less than 1% CPU and 0.1% memory consumed by the Dumpcap process, Figure 16.

[19] Tshark manual page: https://www.wireshark.org/docs/man-pages/tshark.html

[20] Dumpcap manual page: https://www.wireshark.org/docs/man-pages/dumpcap.html

[21] Appendix B: Data Volume Experiment

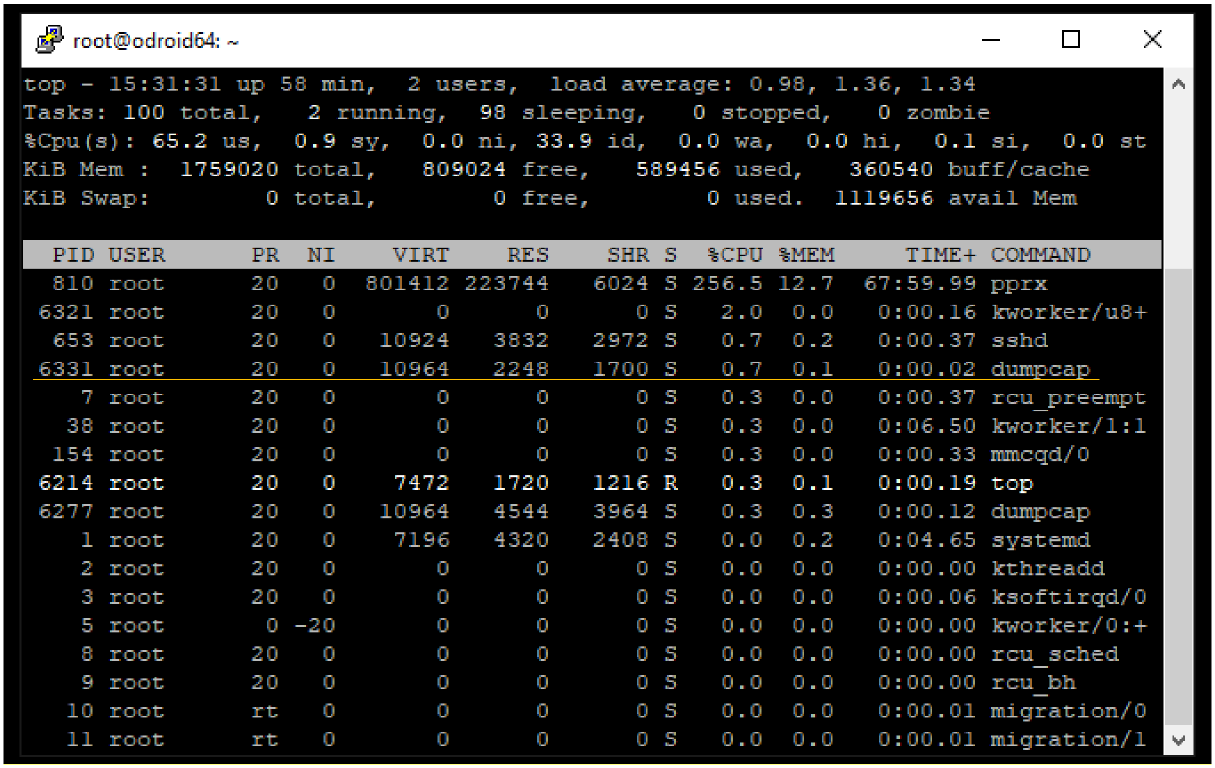


Figure 16: Dumpcap resource utilization while logging **Image Data Stream** (dumpcap) and raw GNSS observations (pprx), in shallow water (sidescan range < 50m).

## 3.3 Optimizing Sidescan Range

A sidescan system's range resolution, or ability to discriminate between two adjacent targets in the across-track direction, is a function of the bandwidth of the pulse, the pulse length and transmit frequency (Figure 17). However, in the case of the Garmin GCV-10 (and recreational sidescan systems in general) the end-user is given little control over these parameters, besides the option to toggle between two very high frequency settings. Instead, the system is designed to automatically optimize these settings to produce the highest possible image resolution regardless of water depth.

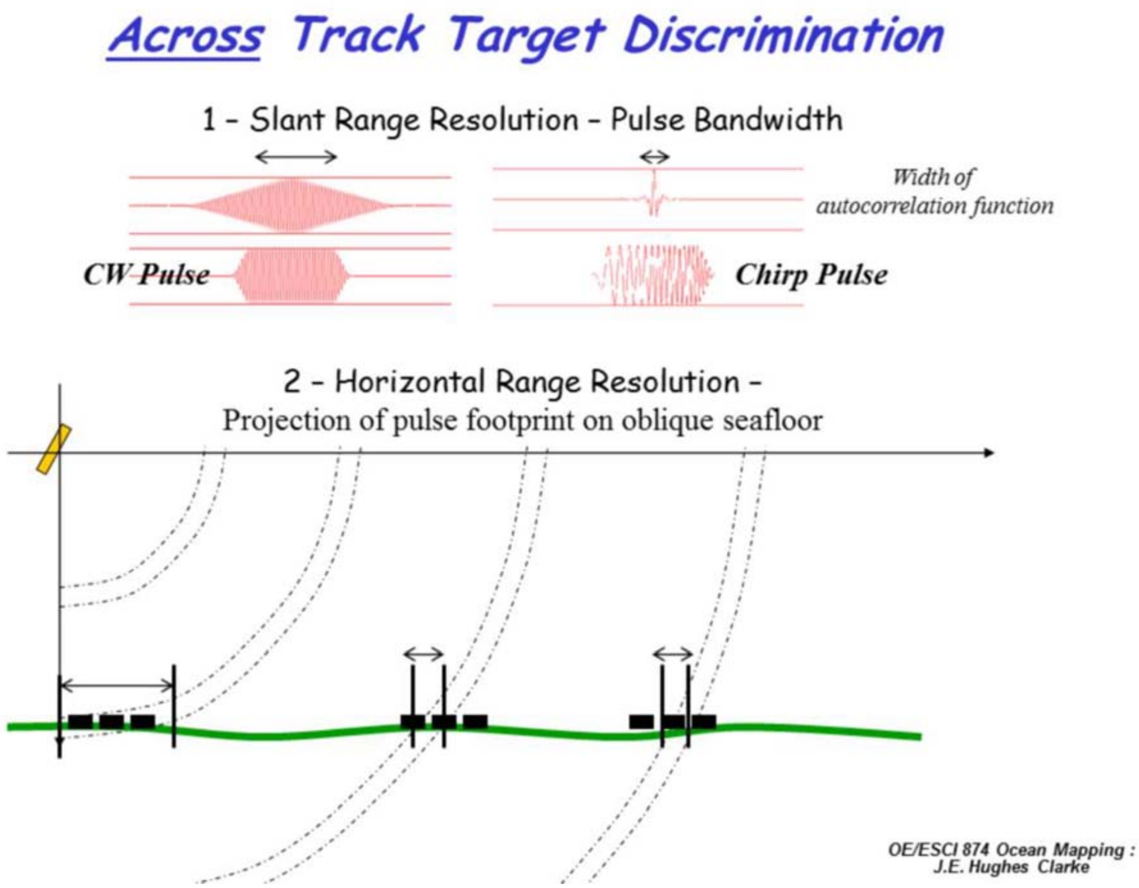


Figure 17: Range resolution model for a sidescan sonar system (Hughes Clarke, 2016). Higher slant range resolution is achieved with physically shorter pulses at a given frequency, or by utilizing chirp pulses which sweep through a band of frequencies, thus dramatically increasing range resolution by decreasing the width of the autocorrelation function. Horizontal range resolution is a function of grazing angle and increases with distance from nadir.

Ideally, a sidescan equipped TCB system would take advantage of the manufacturer's optimization algorithm by imaging targets in automatic range mode unless, for example, a HO wanted to apply a manual range setting in hopes of increasing along track resolution in a high-speed area, or to attempt to image a target far abreast of the marked channel. However, attempts to determine if, or where, the GCV-10 reports the range settings in the imagery data stream were unsuccessful. The impact of this problem is that it is impossible to build a properly georeferenced sidescan record in XTF format, without knowledge of the range setting associated with each scanline. To overcome this problem the range setting was manually controlled for the remainder of this work.

To determine the most appropriate range settings to manually apply, R/V *Gulf Surveyor* was used to navigate the Garmin GCV-10 to locations that exhibit the approximate range of water depths available in the Piscataqua River, where future testing would take place (Figure 18). At each of these depth zones, the GCV-10 was allowed to automatically adjust its sidescan range setting, and the setting was recorded (Figure 19). Since a primary intention for a TCB implementation of this technology is to enable a vessel to record a stand-off acoustic image of a hydrographic target of interest, without endangering the vessel with the need to pass over the top, this experiment was conducted using the lower frequency (455 kHz) setting to maximize scan range.

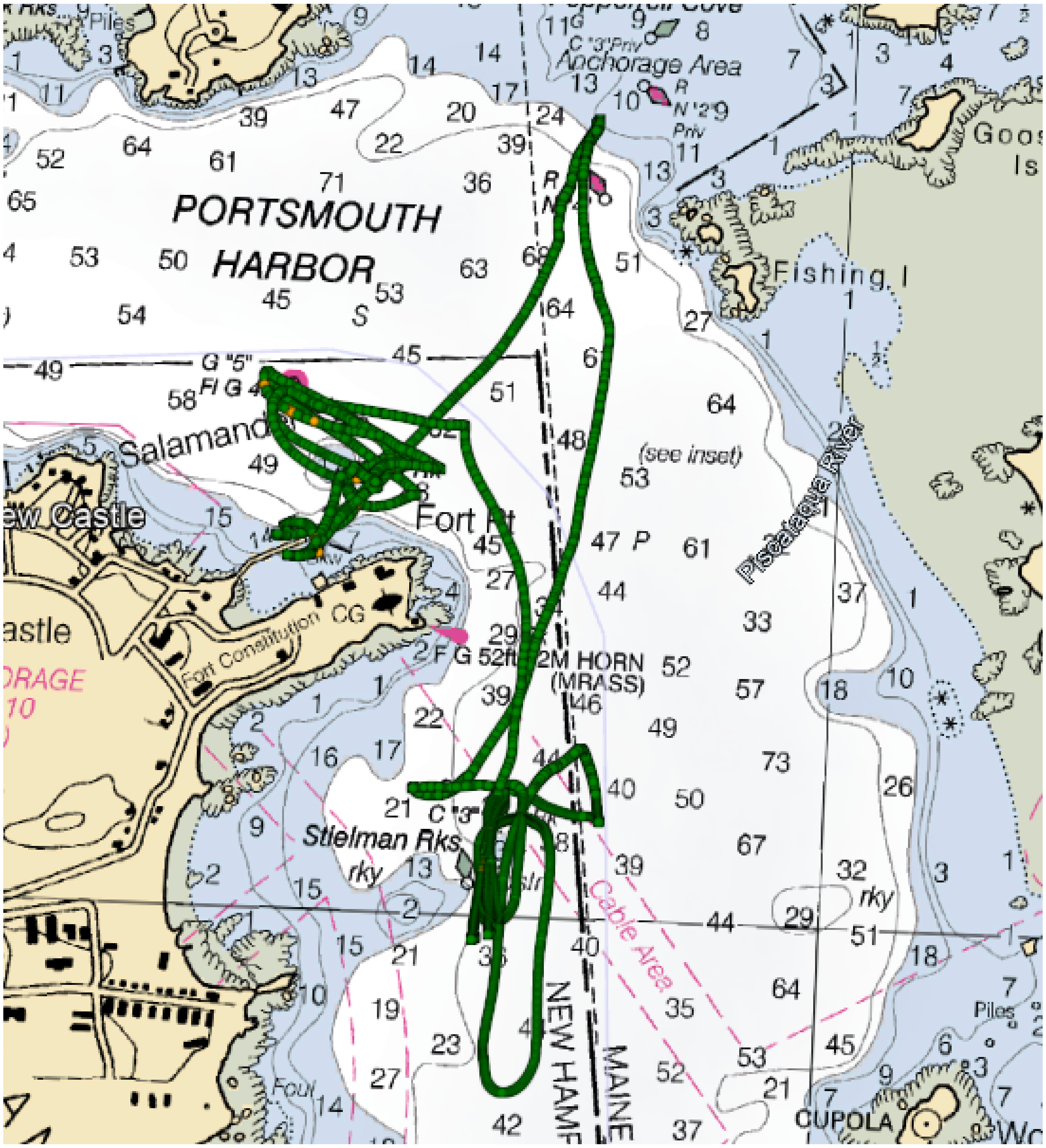


Figure 18: RVGS navigation record overlaid on NOAA Chart 13283 from data collection in the Piscataqua River to determine the Garmin GCV-10's optimized sidescan range setting in varying water depths.

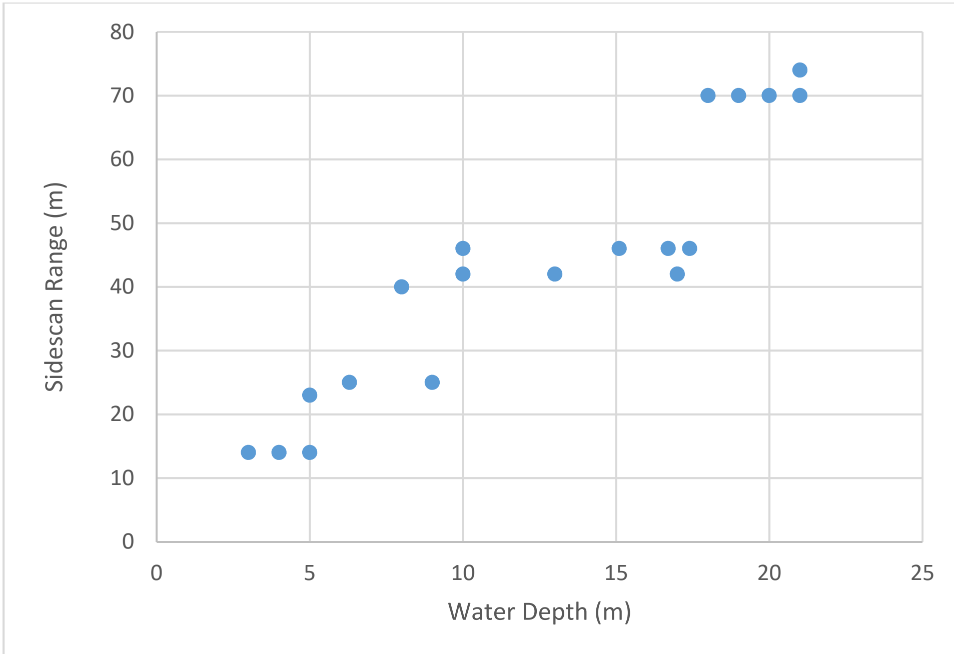


Figure 19: Automatic sidescan range settings applied by the Garmin GCV-10 in water depths between 3-21 meters at 455 kHz CHIRP.

The results of this experiment show the Garmin GCV-10 automatically adjusts its range to 3-5x water depth in the depth regime considered. The adjustment is closer to 5x water depth in the shallows and decreases to approximately 3x water depth in deeper water. These results were used to define the range settings used to autonomously image sidescan targets in section 3.5.3.

## 3.4 Determining the System Latency

In hydrography, the system latency is the difference in time between two different data sources, usually between navigation and sonar data. It is specifically tied to the difference between the clocks on these two systems, and the point at which each system applies a timestamp to the data. Failing to compensate for the latency results in a systematic positioning error in a georeferenced sonar record because the time tag associated with a received echo is offset from the navigation system's time. This timing offset may be static or dynamic, depending on the system.

To produce precisely georeferenced sidescan imagery, a component of the total system latency was quantified in the following desktop experiment[22]. This component is the latency associated with the time in which the transducer senses the returned echo, to the time in which the observation is timestamped in the digital sidescan record.

The embedded Odroid computer in the TCB datalogger keeps time with a local oscillator, which is disciplined to UTC time by the system's integrated GNSS receiver using Network Time Protocol (NTP), (Mills, 1992). When the datalogger is recording the **Image Data Stream**, each datagram is UTC time tagged by the datalogger's clock. This is the time the digitized datagram was recorded. However, the latency must be determined by comparing the time the digitized datagram was recorded to the time the transducer received the returned echo.

Since defining the precise time, the GCV-10 transducer senses an incoming soundwave is not trivial, this experiment used a physical tap of a finger against the transducer face as an analog to an incoming acoustic pulse to record the exact time a finger covers the transducer face. A free GPIO pin on the TCB datalogger board was used to facilitate a pull-up resistor circuit (Figure 20). The circuit can be completed by using a finger to tap a floating bare wire against a bare wire fastened to the transducer face (Figure 21). Therefore, completing the circuit triggers two events. 1) The **Image Data Stream** records the digitized tap in the sidescan record (Figure 22). 2) The GPIO pin registers a low voltage state and triggers a system interrupt with an associated time tag. The difference between the timestamp of the first datagram received for a given 'tap', and the

[22] Full experimental procedure in Appendix C: Desktop Latency Experiment Procedure

timestamp of the associated system interrupt, is an estimate of the system latency associated with digitizing the sidescan record.

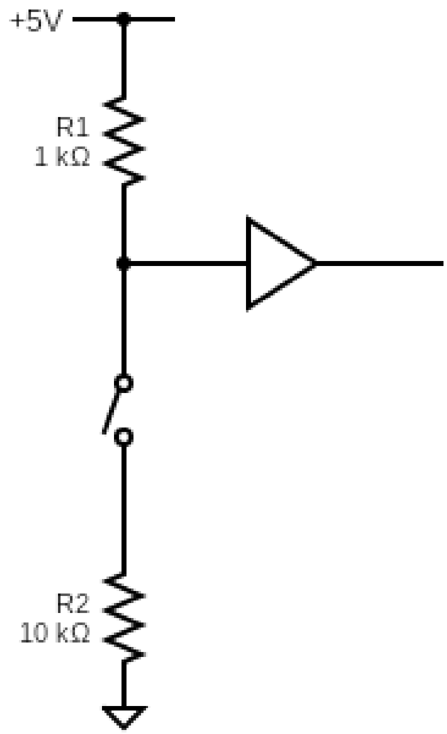


Figure 20: Pull-up resistor circuit diagram. The TCB datalogger utilizes an Odroid C2 computer capable of 5VDC output on Pin 1. Header pin #16 (GPIO #236) registers LOW when the circuit is completed at the transducer.

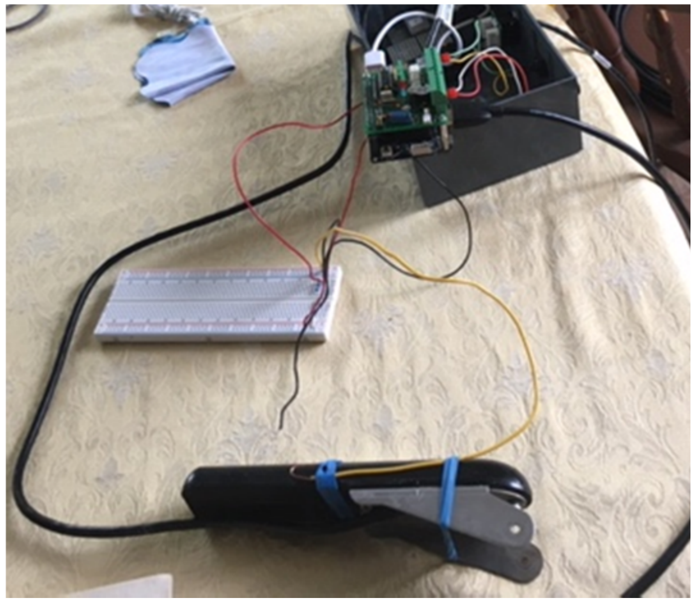

Figure 21: Pull-up resistor circuit implementation. The Odroid C2 computer with SeaID GNSS receiver was removed from the case to provide access to the Odroid's I/O pins.

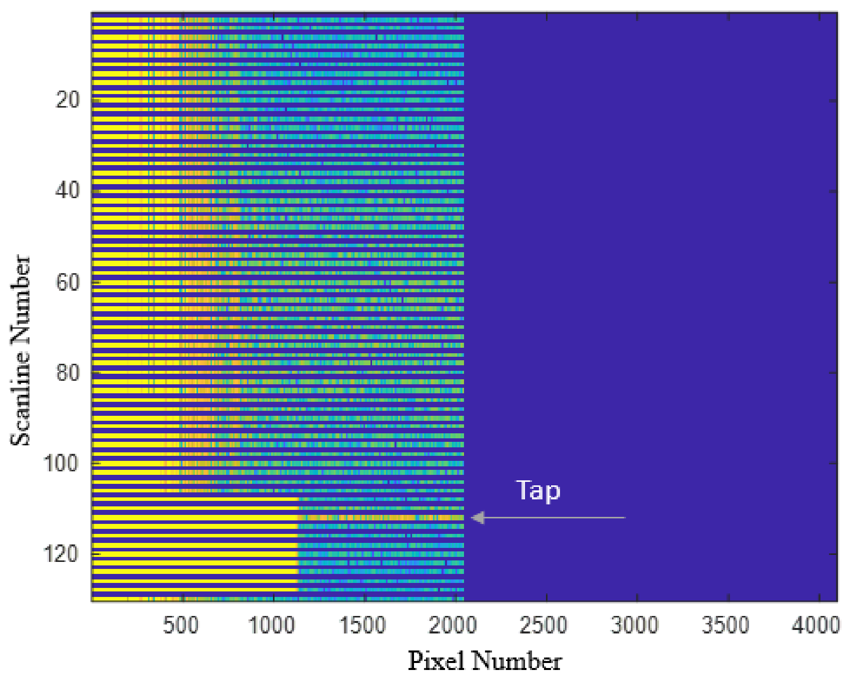


Figure 22: Transducer tap visualized in a reconstructed sidescan record using custom MATLAB code. Only the portside data is visualized because the starboard side of the transducer was face-down on the table, making the data irrelevant.

It was theorized that the system latency may fluctuate as a function of the GCV-10's range setting. Therefore, the system latency was quantified (n=50) with the range manually set to 3, 50, 100, and 200 meters, which characterize the breadth of range settings the system is capable of at 455kHz. At broader range settings a tap would oftentimes register as several scanlines, Figure 23. When this occurred, the timestamp associated with the first datagram received from the first scanline was used for the calculation.

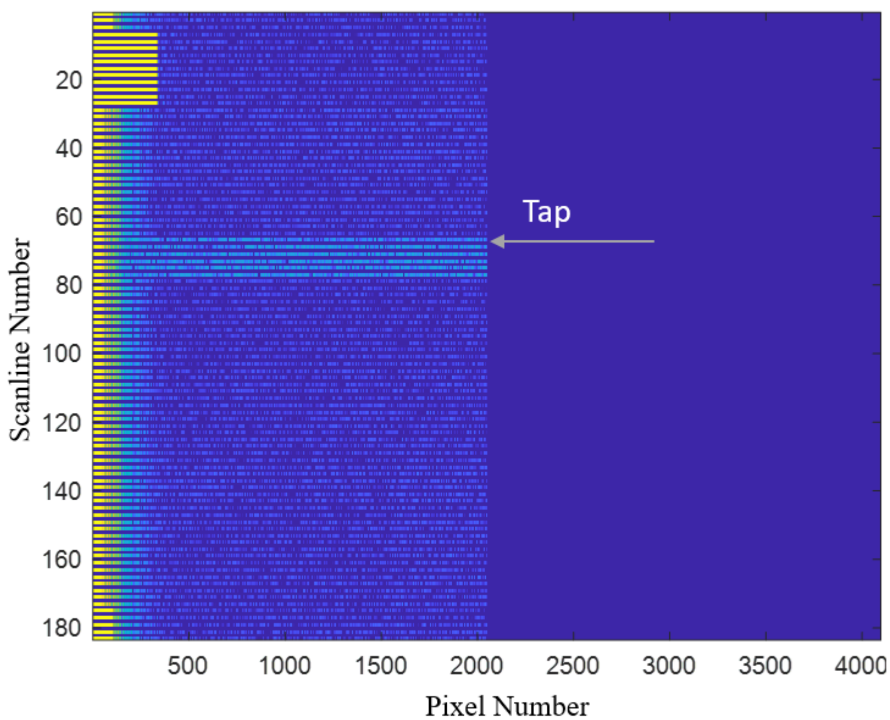


Figure 23: Latency test run at 200-meter sidescan range. Notice the transducer tap is registered as multiple scanlines.

A probability density function of the system latency was generated with the latency data compiled across each range setting, and across all range settings (Figures 24&25). These results show that the system latency is predictable within ~0.3 seconds and can likely be modeled by a gamma distribution.

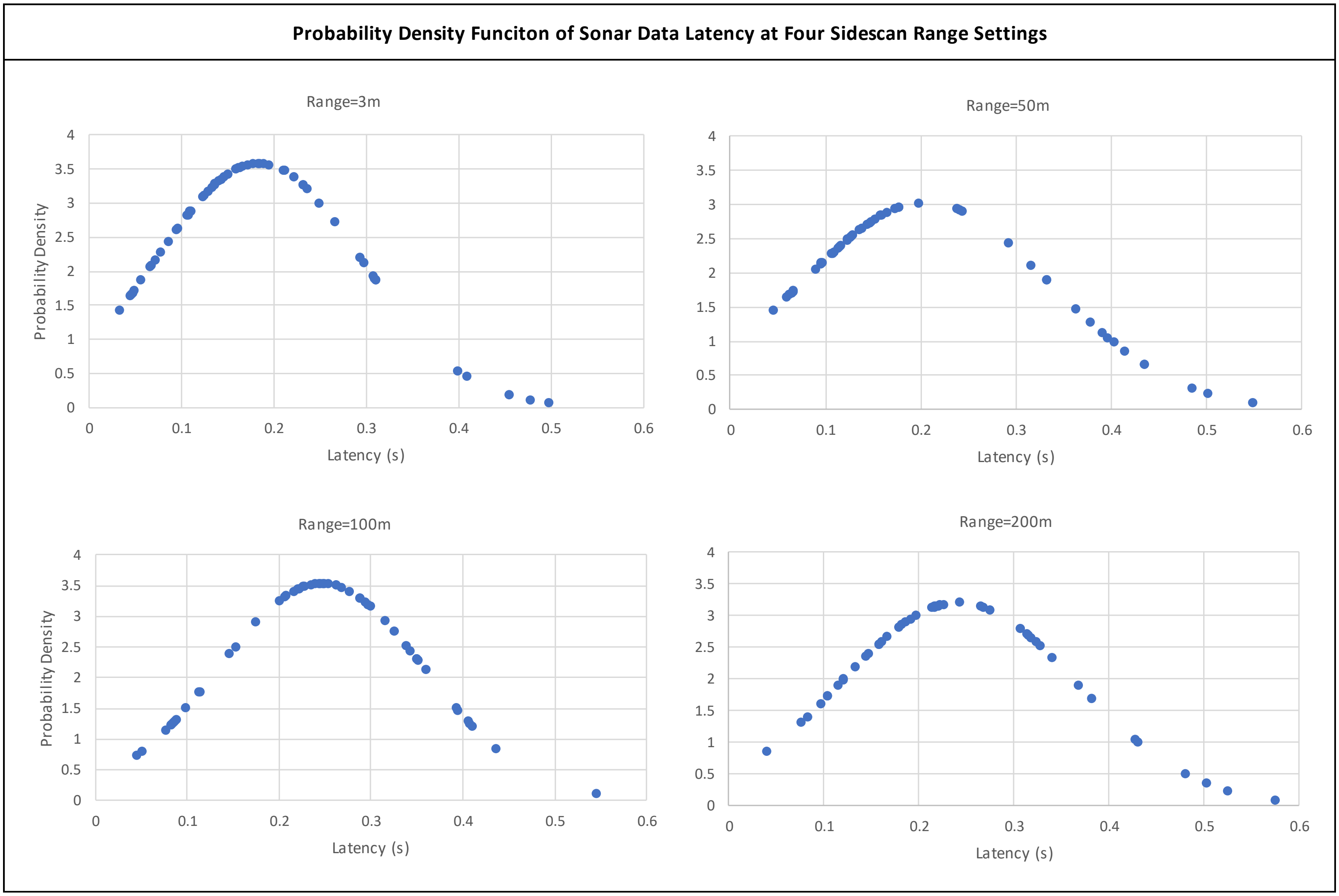


Figure 24: Probability density function of Garmin GCV-10 digitization latency at 3m, 50m, 100m, and 200m sidescan range.

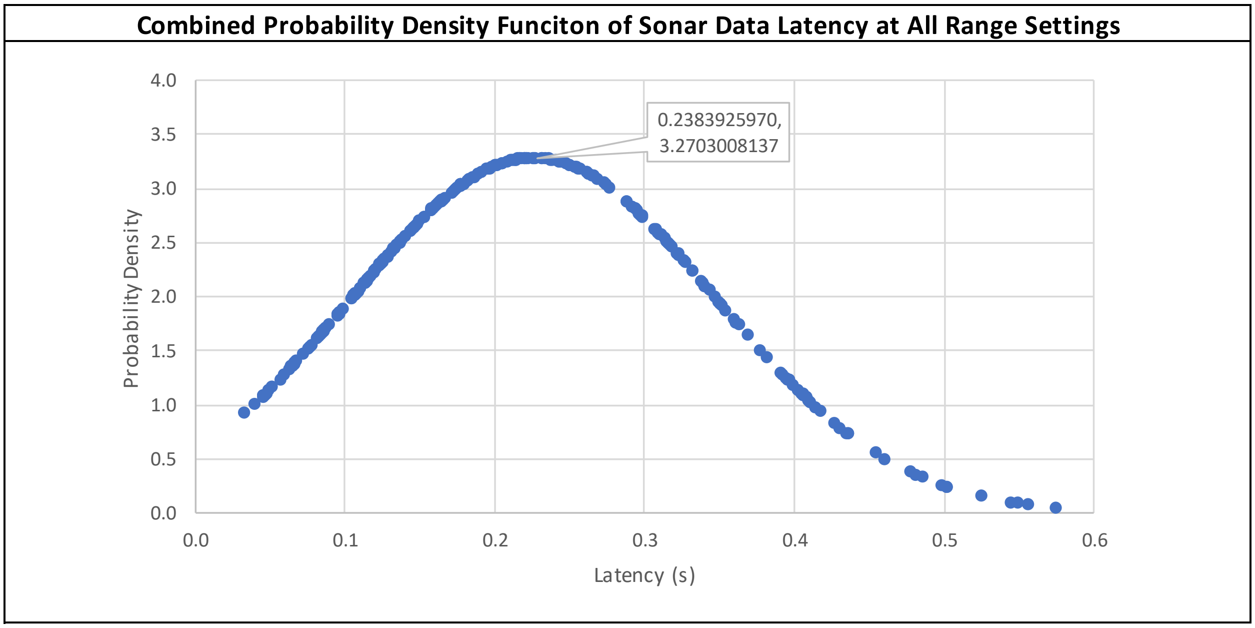


Figure 25: Probability density function of the system latency associated with digitizing Garmin GCV-10 sidescan data and storing it on the TCB datalogger computer. Sidescan range set at 3, 50, 100, 150 and 200 meters. N=257

The system latency shows some dependence on range setting, as, latency increases by ~50ms at 100m or greater range (Figure 24). However, the magnitude of this difference is small, and would imply a 0.10m bias at 4 knot speed over ground, or a 0.20m bias at 8 knots. The system latency was estimated as 0.24s to represent the peak of the probability density function at all range settings for the remainder of this work (Figure 25). In section 3.5.2, an underway field test is conducted at 4 and 8 knot vessel speed over ground to verify the results of this experiment using a traditional hydrographic patch test approach.

## 3.5 Autonomously Imaging Sidescan Targets in the Field

In practice, TCB hardware must operate autonomously to remove the burden of stewardship from the vessel operator, and to reduce the likelihood of data loss or corruption due to user error. This section details the evolution of installing the prototype TCB system on R/V *Gulf Surveyor* and demonstrates the concept of operations presented in Section 1.3.3, in which a TCB datalogger may carry a series of waypoints for hydrographic targets of interest, autonomously detect when the vessel is within sidescan range of a target, apply appropriate sidescan settings, and log sidescan imagery as the vessel transits the area.

### 3.5.1 Hardware Installation

The TCB datalogger, Harxon GPS500 antenna, and Garmin GCV-10 were installed on R/V *Gulf Surveyor*, (Figure 26). Since the TCB datalogger can only be monitored and controlled using the Ethernet adapter on the front panel, a laptop was configured with an SSH client to enable access to the datalogger's command line interface. The laptop and TCB Datalogger were assigned static IP addresses on the GCV-10's subnet so traffic could be routed through the built-in switch.

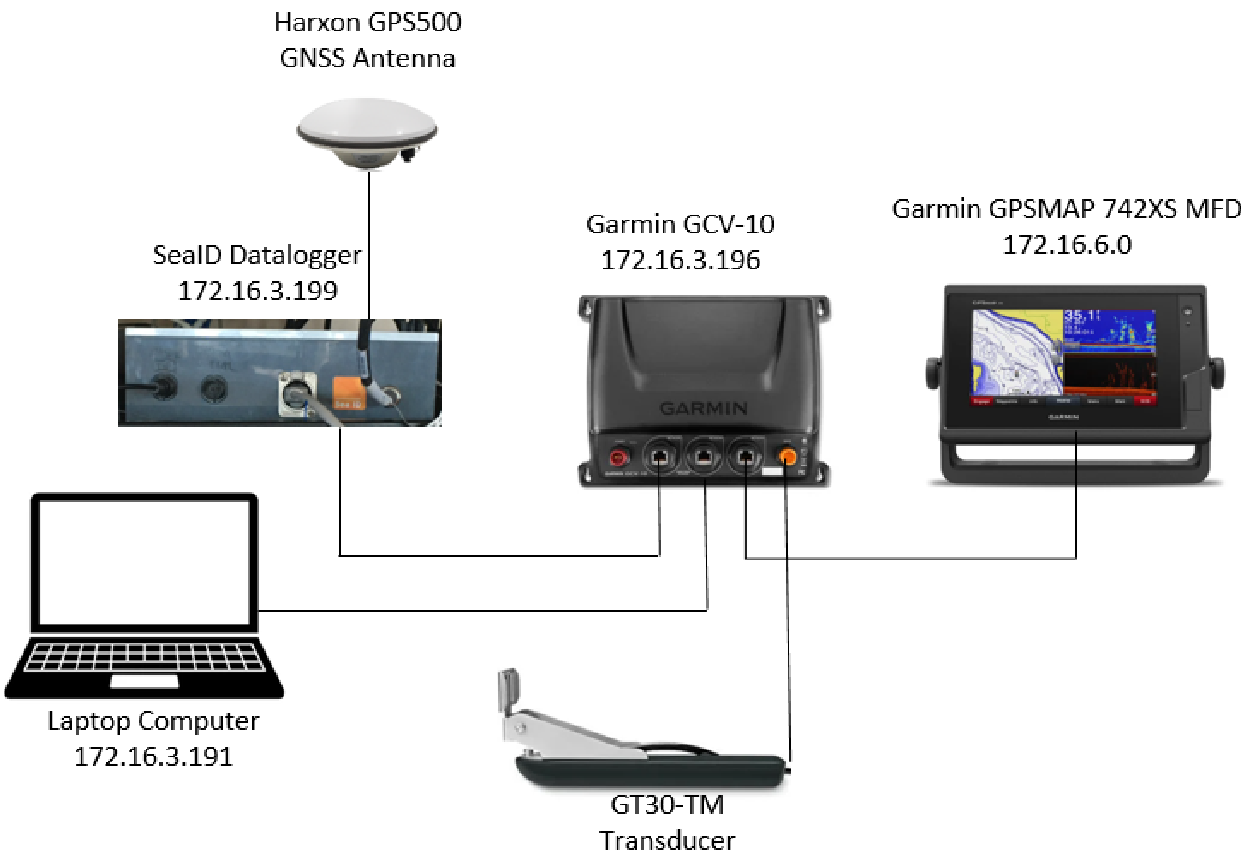


Figure 26: Hardware installation topology.

The Harxon GPS500 antenna was mounted on one of the vessel’s auxiliary antenna mounts with a clear sky view, and an impedance matched (50 Ω) antenna cable was routed from the antenna to the datalogger, (Figure 27).


Figure 27: Harxon GPS500 antenna installed on R/V *Gulf Surveyor*.

The Garmin GT30-TM transducer was installed on the vessel's primary transducer strut and aligned to the vessel's centerline (Figure 28).

Figure 28: Garmin GT30-TM transducer installed on R/V *Gulf Surveyor's* primary transducer strut. The strut is aligned with the vessel's centerline and can be vertically articulated from the stowed position (shown), to a deployed position which secures the transducer submerged below the hull, clear of bubble wash.

The Garmin GCV-10, TCB Datalogger, and GPSMAP 742XS were mounted in R/V *Gulf Surveyor's* electronics rack and connected to a 12VDC power supply. The GPSMAP 742XS was simply used to confirm echosounder settings were properly applied by the TCB Datalogger, and to provide the vessel operator a real-time sidescan data display (Figure 29). Efforts were made to develop a real-time sidescan display using custom MATLAB code, but these efforts were abandoned due to the impracticality of reassembling UDP datagrams without significant packet loss in a high-level programming language. Code translation to a lower-level language to improve speed was not pursued because it is unlikely a vessel of opportunity would carry a Garmin GCV-10 without a topside unit. If there is interest, perhaps from a HO, to outfit several vessels with a sidescan capable TCB system, it would be possible to lower the total hardware cost by eliminating the need for a Garmin MFD[23], while retaining the value that a real-time display provides the vessel operator.


Figure 29: 12VDC Power Supply, Garmin 742XS multifunction display and TCB Datalogger installed on RVGS.

[23] The Garmin 742XS MFD used in this research retails for ~$1000, representing significant opportunity for cost saving.

### 3.5.2 Field Testing Latency Compensation

To prove the system latency was properly quantified by the desktop experiment, two conspicuous sidescan targets were imaged with a constant heading at 4 and 8 knot vessel speed over ground using the TCB system installation onboard R/V *Gulf Surveyor* (Figure 30).


Figure 30: Satellite imagery overview of two locations, A and B, where field latency tests were conducted in the vicinity of the UNH Pier Facility in New Castle, New Hampshire.

At site 'A' the mooring chain for USCG buoy GC'3' was imaged using the TCB Datalogger to send commands to configure the Garmin GCV-10 to collect sidescan imagery at 800 kHz with a 40-meter swath width. These settings were chosen to maximize the resolution of the imagery, as the 800 kHz setting maximized the impedance contrast of the chain, and a 40-meter swath allowed the vessel to pass a safe distance from the target position while minimizing the scan range and maximizing along-track resolution. At site 'B' the same methods were used to image the seafloor and dock pilings around the New Hampshire State Port Authority at 455 kHz with a 40-meter swath width.

Once data collection was complete, GNSS observations were halted. The raw observations were filtered for the appropriate satellites and converted from the logger's native binary format to RINEX format, using custom code provided by SeaID.

RINEX files were post-processed in RTKLib using the rapid ephemeris, with the NOAA Continuously Operating Reference (CORS) station installed on the UNH campus as a base station[24], and with the receiver in kinematic positioning mode. The output file provides Earth Centered Earth Fixed (ECEF) coordinates at 1Hz with horizontal uncertainty <5cm and vertical uncertainty <1cm[25]. Positions are reported in the World Geodetic System 1984 (WGS84) datum. Data processing was completed according to Appendix B: Processing Data from Field Collection.

The MATLAB code, PARSER_Master, was used to reassemble the sidescan imagery and find the timestamp associated with the first packet received from each scanline. The system latency was then corrected by subtracting 0.24 seconds from this epoch per the results of the desktop latency experiment. Finally, the precise position associated with each scanline epoch was calculated using linear interpolation.

Reassembled sidescan imagery with post-processed positions associated with each scanline epoch were then input to xtf_converter_tcb.py which converts the data to XTF file format for viewing in hydrographic software packages (Figures 31&32).

---

[24] CORS station NHUN: https://geodesy.noaa.gov/cgi-cors/corsage_2.prl?site=NHUN
[25] RTKLIB Output File in Appendix C: Field Test Latency Processing

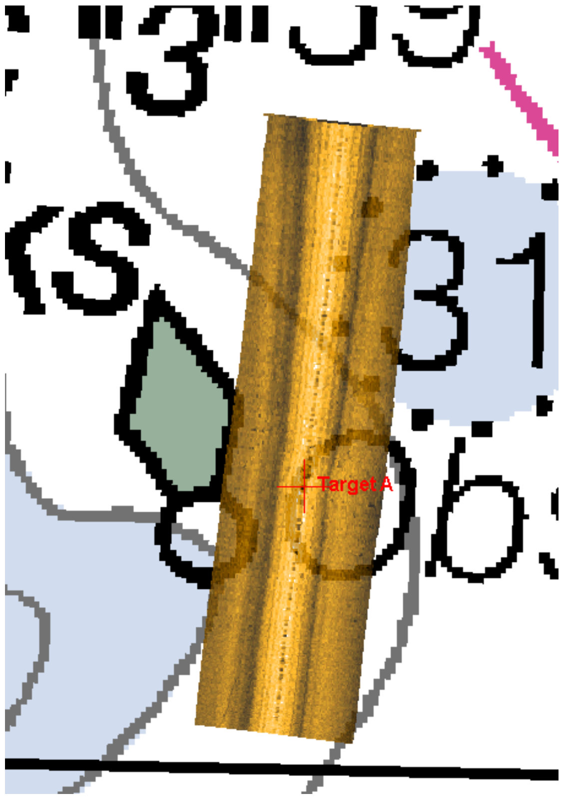


Figure 31: Georeferenced sidescan record with water column removed from latency test site A, overlaid on NOAA chart 13285 (top). Sidescan waterfall display from latency test site A, notated with gridlines at 1m interval for scale (bottom). The target position used for the test is notated in both images.

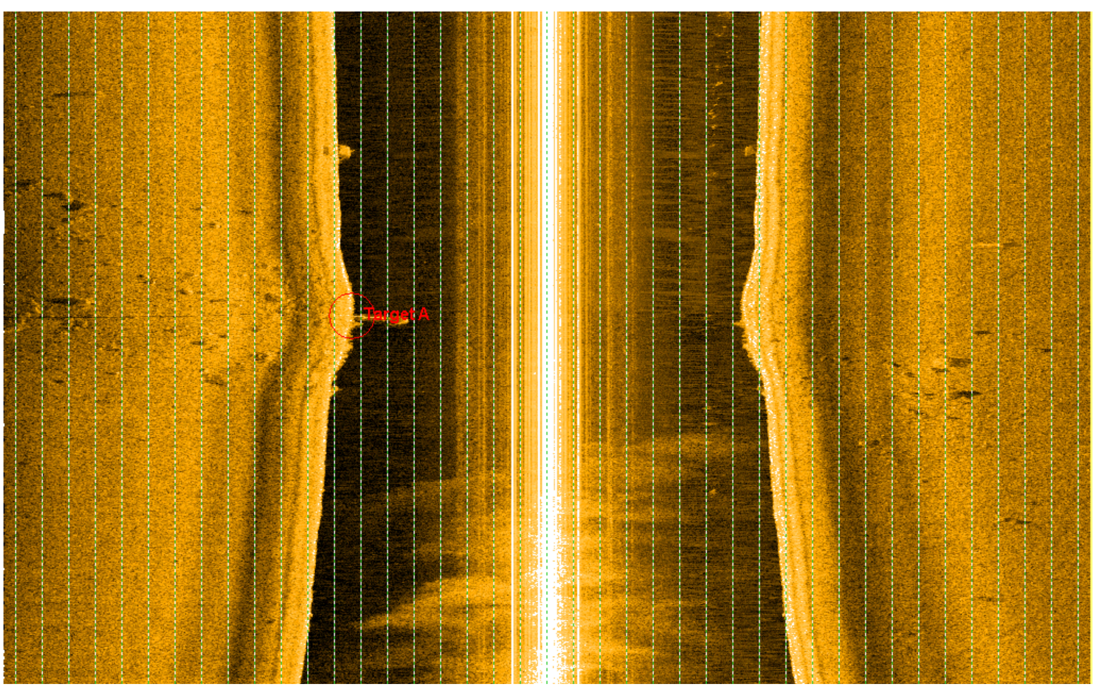

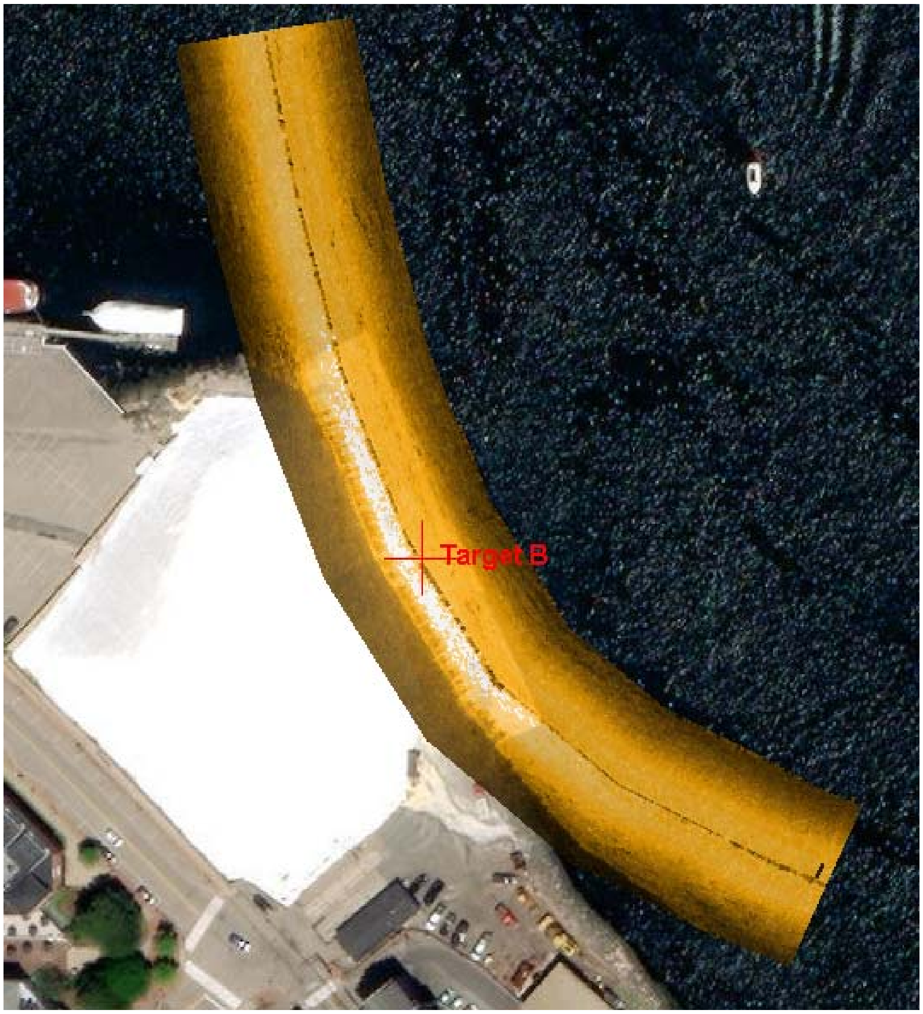


Figure 32: Georeferenced sidescan record with water column removed from latency test site B, overlaid on satellite imagery. Associated sidescan waterfall display, notated with gridlines at 1m interval for scale (bottom). The target position used for the test is notated in both images.

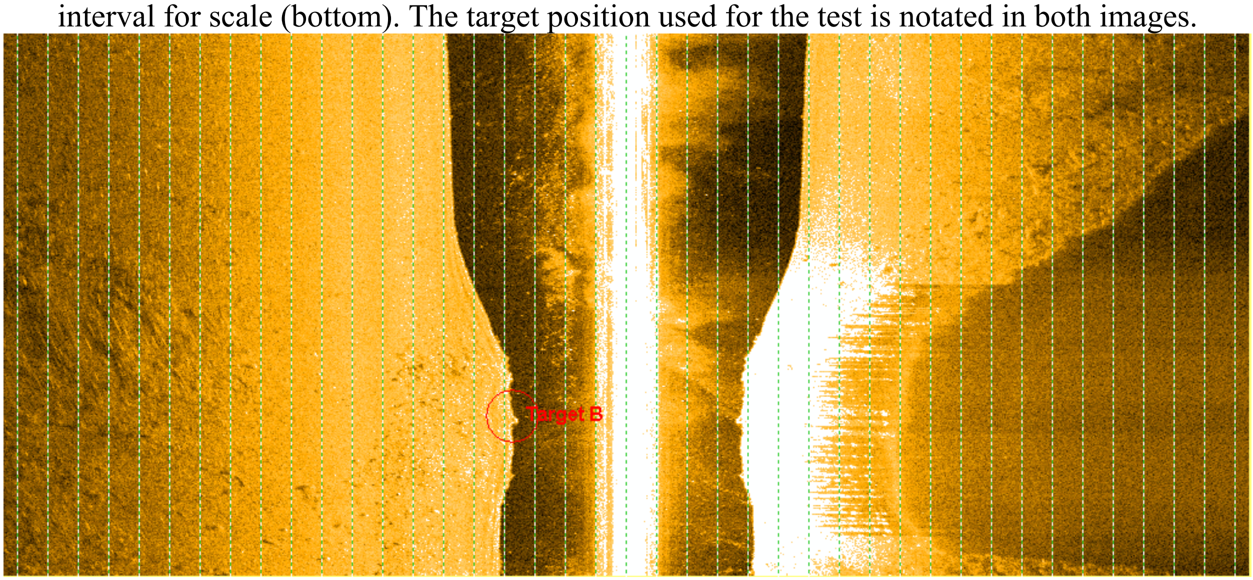

At both test sites, the reported target position did not vary significantly (<1 meter) with vessel speed, indicating system latency has been properly assessed and is not a significant source of positioning error, Figure 33.

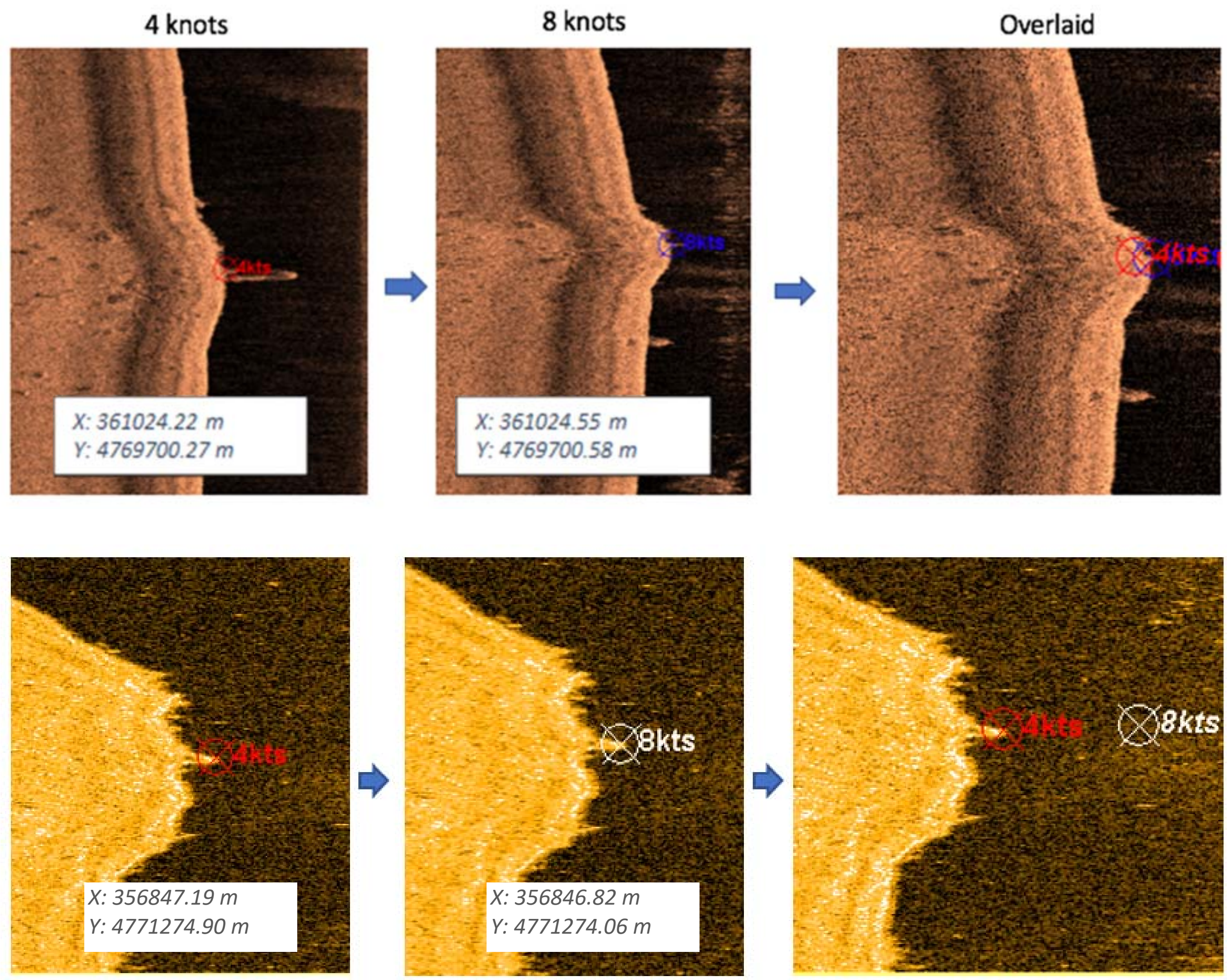


Figure 33: Latency test targets imaged at 4 and 8 knots over ground at site A (Top), and B (Bottom). Target positions are notated in Earth Centered Earth Fixed (X,Y,Z) coordinates. At site A, the declared position of the base of the mooring chain varies by ~30cm in the horizontal (XY) plane when vessel speed is doubled. At site B, the position of a conspicuous bathymetric feature varies by ~80cm in the horizontal (XY) plane. The Z-coordinate is ignored because sidescan sonar systems are fundamentally unable to determine target depth.

The small horizontal position uncertainties (<1m) observed at both test sites were likely to be caused by a combination of factors including the vessel crabbing due to strong (3-4 knot) tidal currents in the Piscataqua River during data collection, sound speed errors, or distortions caused by the system geometry. Figure 33 supports this hypothesis in showing most of the discrepancy between target positions is in the across-track direction, which is not indicative of a latency error.

Future work should include a detailed analysis of small targets in the sidescan record to determine the probable cause of the uncertainty. This could include integrating data from a heading source to show that correcting for the discrepancy between course over ground and heading will cause the sidescan geometry to change.

### 3.5.3 Demonstrating a Concept for Autonomous Operation

The TCB Datalogger was configured to autonomously operate the Garmin GCV-10 sidescan module by leveraging the code, monitor_realtime_position.py, to monitor the GNSS receiver's reported position, and send commands to the Garmin GCV-10 when the TCB vessel is within a defined proximity to a coordinate defining a hydrographic target of interest. To do this, the code constantly monitors a plain-text file which is automatically generated in the GNSS data capture directory. This file provides access to real-time information from the GNSS receiver including the real-time 3D position of the antenna phase center, or reference point, in Earth Centered Earth Fixed (ECEF) format (Figure 34).

```
==========   GRID: General Radionavigation Interfusion Device    ===========
 Receiver time:     0 weeks  12142.1 seconds        Build ID:        3406
 GPS time:      2103 weeks 171607.0 seconds
---------------------------------------------------------------------------
CH  TXID    Doppler       BCP          PR       C/N0    Az      El   Status
             (Hz)       (cycles)     (meters)  (dB-Hz) (deg)  (deg)
---------------------------- GPS_L1_CA_PRIMARY ----------------------------
 1    2       728.2    -7108490.7   20677289.6  51.4   299.8   63.0     6
 2    4      -810.2       64585.6   23284676.7  38.0    52.9   17.7     6
 3   --   ---------  ------------  -----------  ----   -----  -----    -
 4   17     -2871.9    10753695.2   21959477.3  46.1   127.2   31.1     6
 5   19     -2481.0    -1160949.6   20528605.8  49.2   122.3   51.1     6
 6   12      -305.8    -6888168.2   21037849.4  44.1   279.7   42.3     6
 7   25      1385.0    -3400009.4   22548677.0  40.6   310.5   23.4     6
 8    9       955.5    -6162426.2   22304503.9  47.2    88.5   28.3     6
 9    6      -970.2    -5630954.3   19971090.5  51.6    33.1   68.5     6
10   23u      323.1    -4428198.2   22808242.5  42.4    77.9   26.9     6
11   --   ---------  ------------  -----------  ----   -----  -----    -
12    5      3197.9   -10325753.6   21935598.1  48.1   212.4   30.6     6
13   --   ---------  ------------  -----------  ----   -----  -----    -
14   --   ---------  ------------  -----------  ----   -----  -----    -
15   --   ---------  ------------  -----------  ----   -----  -----    -
---------------------------- GPS_L2_CLM_PRIMARY ---------------------------
 1   12      -238.1    -1288595.1   21037838.4  44.4   279.7   42.3     5
 2   --   ---------  ------------  -----------  ----   -----  -----    -
 3    6      -756.0    -5837267.6   19971082.9  53.4    33.1   68.5     5
 4   17     -2238.1     8397571.9   21959464.9  45.9   127.2   31.1     5
 5    9       744.5    -5253014.5   22304494.1  48.6    88.5   28.3     5
 6   25      1079.0    -5314168.9   22548670.1  44.5   310.5   23.4     5
 7    5      2491.8    -7871636.2   21935587.9  47.2   212.4   30.6     5
 8   --   ---------  ------------  -----------  ----   -----  -----    -
 9   --   ---------  ------------  -----------  ----   -----  -----    -
---------------------------- SBAS_L1_I_PRIMARY ----------------------------
 1  138      -195.6     2272858.4   38064229.3  42.3   227.3   28.3     6
 2  125      -303.6     1084382.2   38880175.4  37.8   115.7   16.6     6
 3  131      -193.1      225978.5   38632953.5  40.6   236.8   22.3     6
 4   --   ---------  ------------  -----------  ----   -----  -----    -
---------------------------- GALILEO_E1_BC_PRIMARY ------------------------
 1    7      2638.0    -7534160.4   25466351.1  44.9   155.1   28.0     6
 2    1     -1340.4    -6931061.0   25405463.1  40.5   273.9   30.6     6
 3   26      1090.9   -12795860.1   22594119.9  50.4   301.0   53.3     6
 4    8       561.7   -11387148.9   22424769.7  48.5    92.0   41.8     6
 5    3     -1929.9     3421127.8   26658946.1  40.7    40.2   15.6     6
 6   --   ---------  ------------  -----------  ----   -----  -----    -
 7   --   ---------  ------------  -----------  ----   -----  -----    -
 8   --   ---------  ------------  -----------  ----   -----  -----    -
----------------------------- Navigation Data -----------------------------
 X:  1538213.30   Y: -4404822.67    Z:  4334192.00   deltRx:     -690254.30
 Xvel:     -0.00   Yvel:      0.03   Zvel:     -0.05   deltRxDot:      36.56
 Hsigma:   0.41   Vsigma:    0.51   NISratio: 0.41
===========================================================================
```

Figure 34: Output of real-time GNSS receiver status file (Display.log) generated by the datalogger. The Navigation Data field shows the calculated position of the antenna in Earth Centered Earth Fixed (ECEF) coordinates as X,Y,Z values.

By generating an imaginary boundary circle around a target of interest with radius equal to 3-5x the charted water depth (per results from section 3.3), the code can determine when the TCB vessel is within reasonable proximity to a sidescan target by defining when the antenna enters or exits a boundary circle. When a boundary is entered, the sidescan is commanded to transmit at a programmed frequency and scan range for a defined period, and to repeat this process until the TCB system registers a position clear of the boundary. In the case the sidescan is already transmitting, as it is being used as a navigation instrument by the host vessel, only the range would be adjusted. Figure 35 provides a visual demonstration of this concept resulting in an automated scan of the UNH Pier in New Castle, NH.

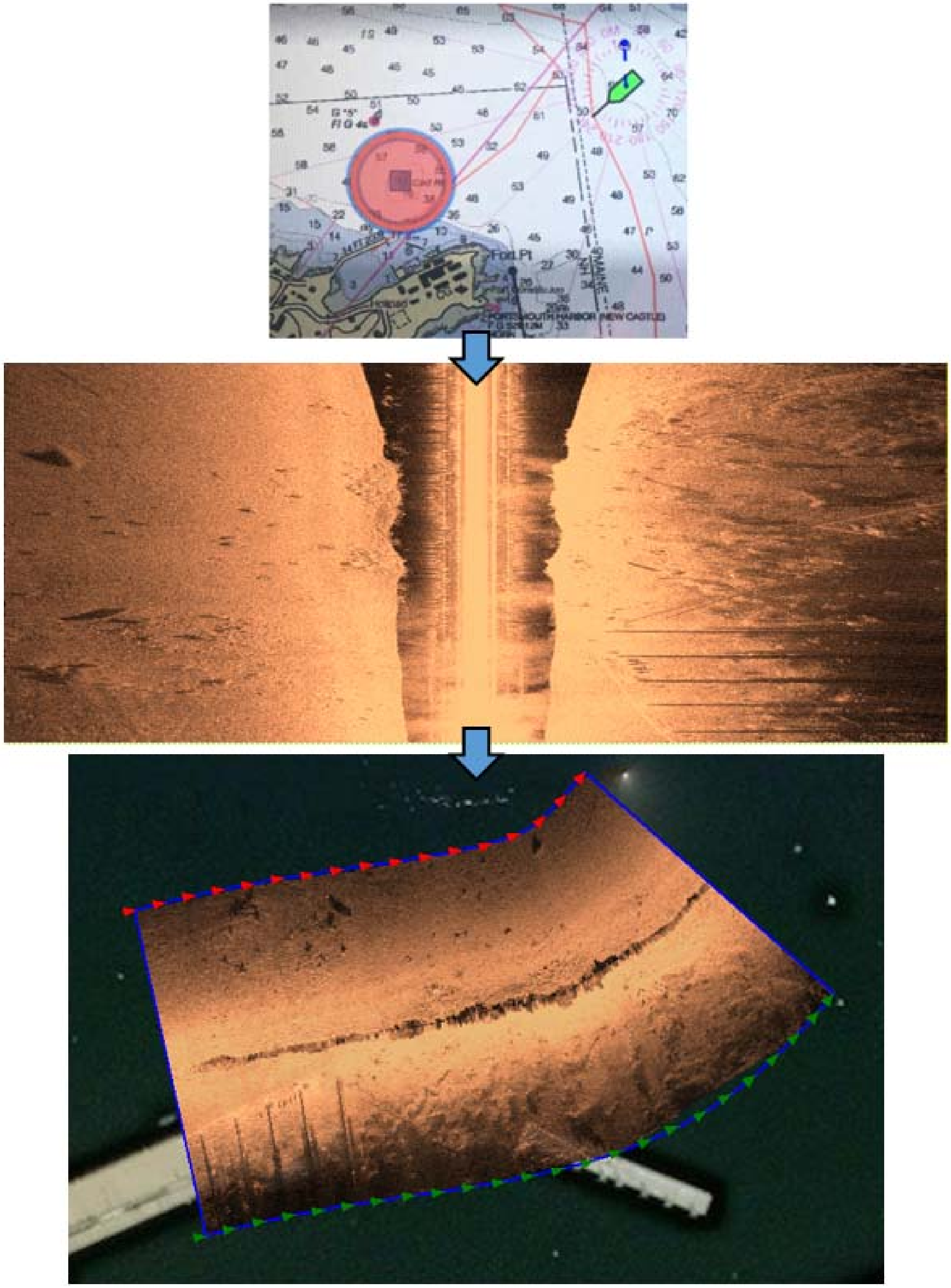

Figure 35: The image on top shows a hydrographic target (marked by a blue square) displayed on R/V *Gulf Surveyor's* chart-plotting software (Rose Point Coastal Explorer). An imaginary boundary zone around the target is displayed by the red circle. The reassembled sidescan waterfall display is shown in the middle image. The bottom image shows the final georeferenced product with water column removed and the horizontal lever arm offset between the transducer and GNSS antenna corrected. Note the artifact from heading misalignment caused by the vessel crabbing due to strong tidal currents most visible in the displacement of the seaward piling on the left-side pier in the sidescan record.

A natural extension to this concept is to define several targets a vessel may image when transiting a particular water body. Consider the following demonstration in Portsmouth Harbor, where four arbitrary sidescan targets were defined and autonomously imaged (Figure 36).

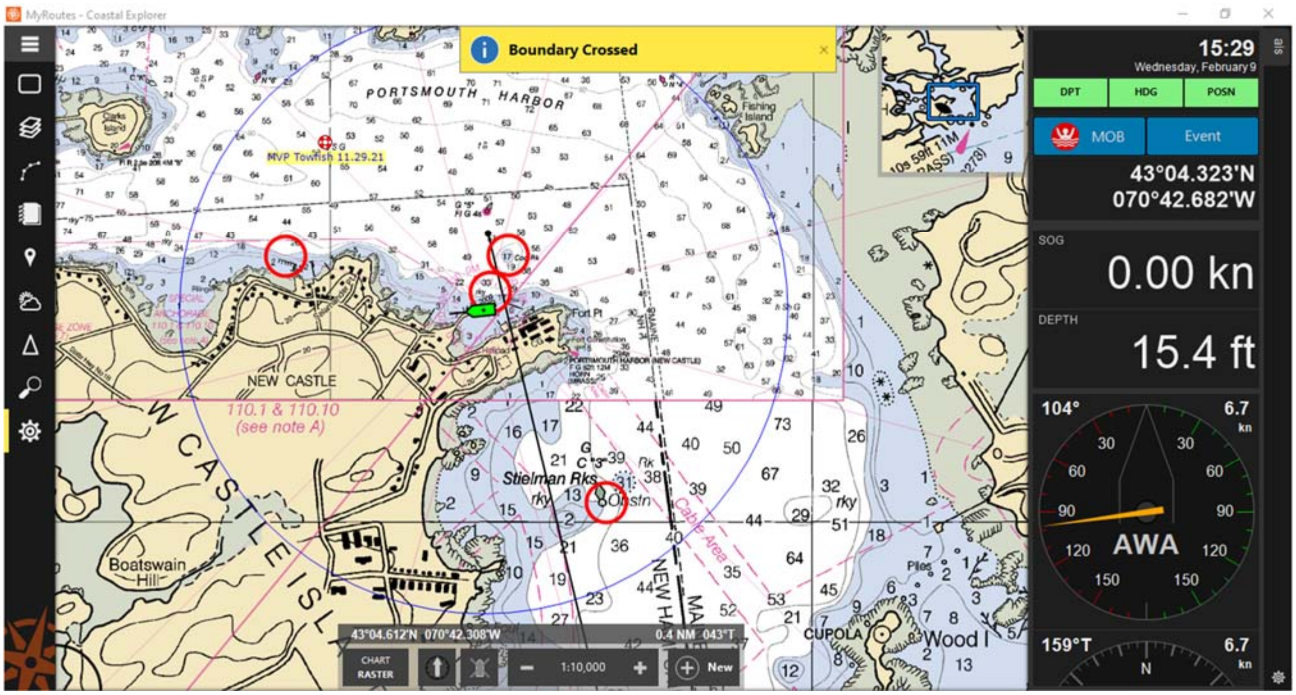


Figure 36: Four boundary circles (red) displayed on *R/V Gulf Surveyor's* chart plotter running Rose Point Coastal Explorer software, marking demonstration targets of interest.

After data collection, the GNSS observations were converted to RINEX format and offloaded in tandem with the sidescan network capture files via FTP connection. The RINEX navigation files were post-processed using rapid satellite ephemeris data[26] provided by the national Crustal Dynamics Data Information System (CCDIS), with the NOAA CORS station (NHUN)

[26] CDDIS data can be accessed online here: https://cddis.nasa.gov/Data_and_Derived_Products/GNSS/orbit_products.html

installed on the UNH campus as a base station, and with the receiver in kinematic positioning mode. These corrected data are made available to the public at zero cost, approximately 17 hours after the end of the previous UTC Day. RTKLIB was used to process these data with the GNSS observations, generating a corrected position record at 1 Hz (Figure 37).

Figure 37: Post processed 3D position solutions from autonomous data collection generated by RTKLIB and visualized in Google Earth. Green dots indicate RTK fix- and yellow dots indicate RTK float-solutions.

Out of the 12,656 solutions shown in Figure 37, 99.3% were high quality PPK (Post-Processing Kinematic) fix solutions with average uncertainties on the order of 2cm on all axes, Table 3.

Table 3: Maximum and mean standard deviations of 3D position solutions post-processed with RTKLIB, displayed in meters.

| **PPK Fix Solution Quality (m)** | |
|---|---|
| Max sd X | 0.0506 |
| Max sd Y | 0.0937 |
| Max sd Z | 0.0705 |
| Mean sd X | 0.009414 |
| Mean sd Y | 0.017487 |
| Mean sd Z | 0.017595 |

The code, PARSER_master.m, was used to reassemble the sidescan imagery, subtract the latency from the timestamp associated with each packet collected from the **Image Data Stream**, and to interpolate the position associated with each scanline epoch. Reassembled sidescan imagery with post-processed positions associated with each scanline epoch were then input to the code, xtf_converter_TCB.py, which converts the sidescan record to XTF file format for viewing in hydrographic software packages. Figure 38 shows the relative locations of four automated scans rendered in the hydrographic software, SonarWiz.

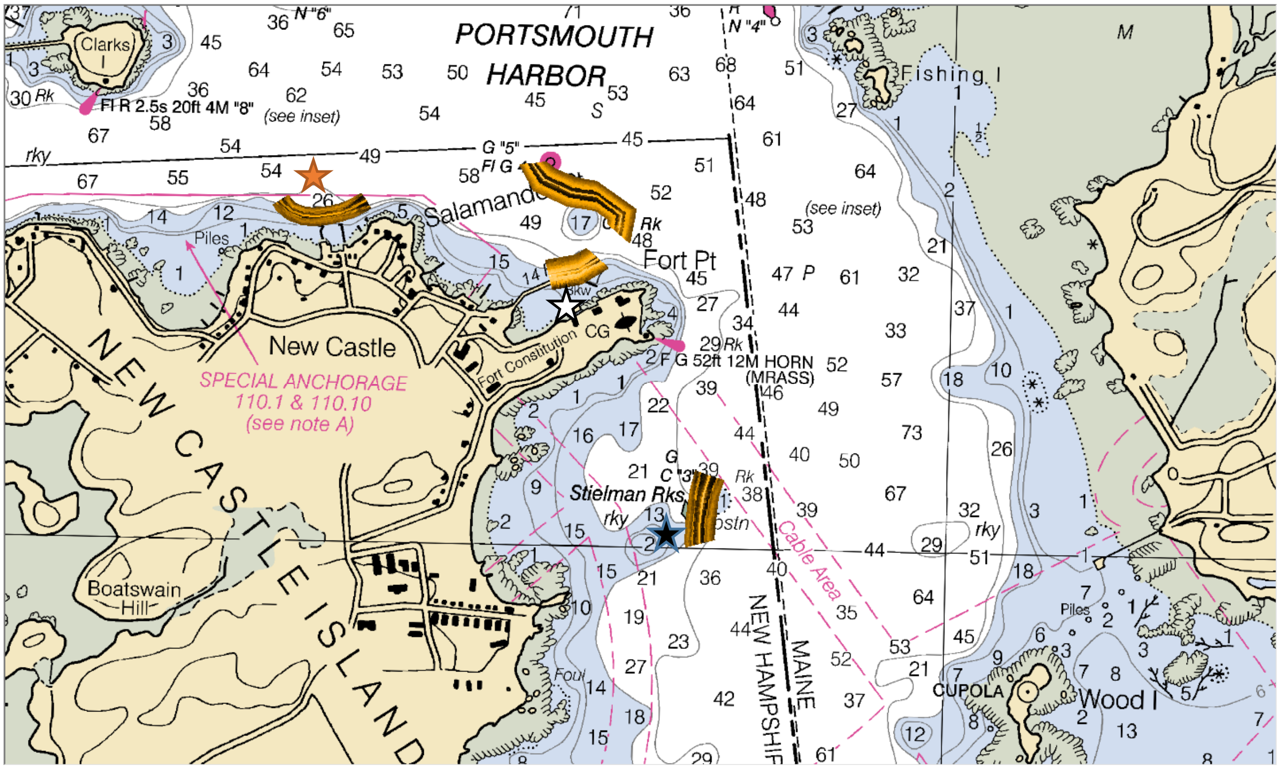


Figure 38: Overview of Garmin GCV-10 sidescan imagery autonomously collected using the TCB datalogger on *R/V Gulf Surveyor's* transit through Portsmouth Harbor. The XTF files are rendered in SonarWiz.

A closer look at the post-processed sidescan files show the impressive imagery generated by the system, and its ability to resolve small targets (<1 square meter) in the water column and on the seafloor. Take for example, the automated scan in the vicinity of Stielman Rocks (Figure 39, 40, 41).

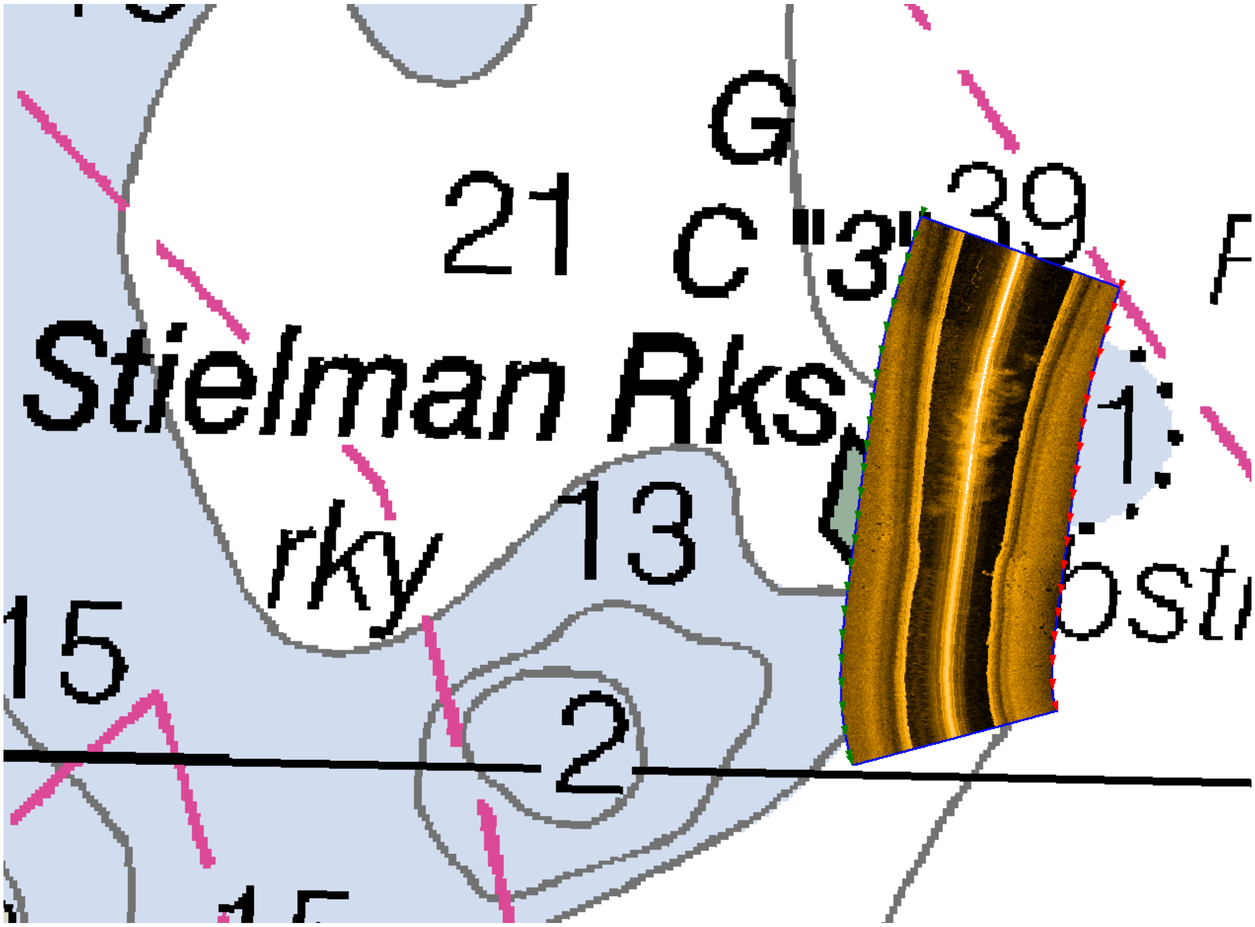


Figure 39: Garmin GCV-10 sidescan record with water column collected at ~4kts, 20m scan range, 800kHz, in vicinity of Stielman Rocks, Portsmouth Harbor, New Hampshire. Overlaid on NOAA chart 13283.

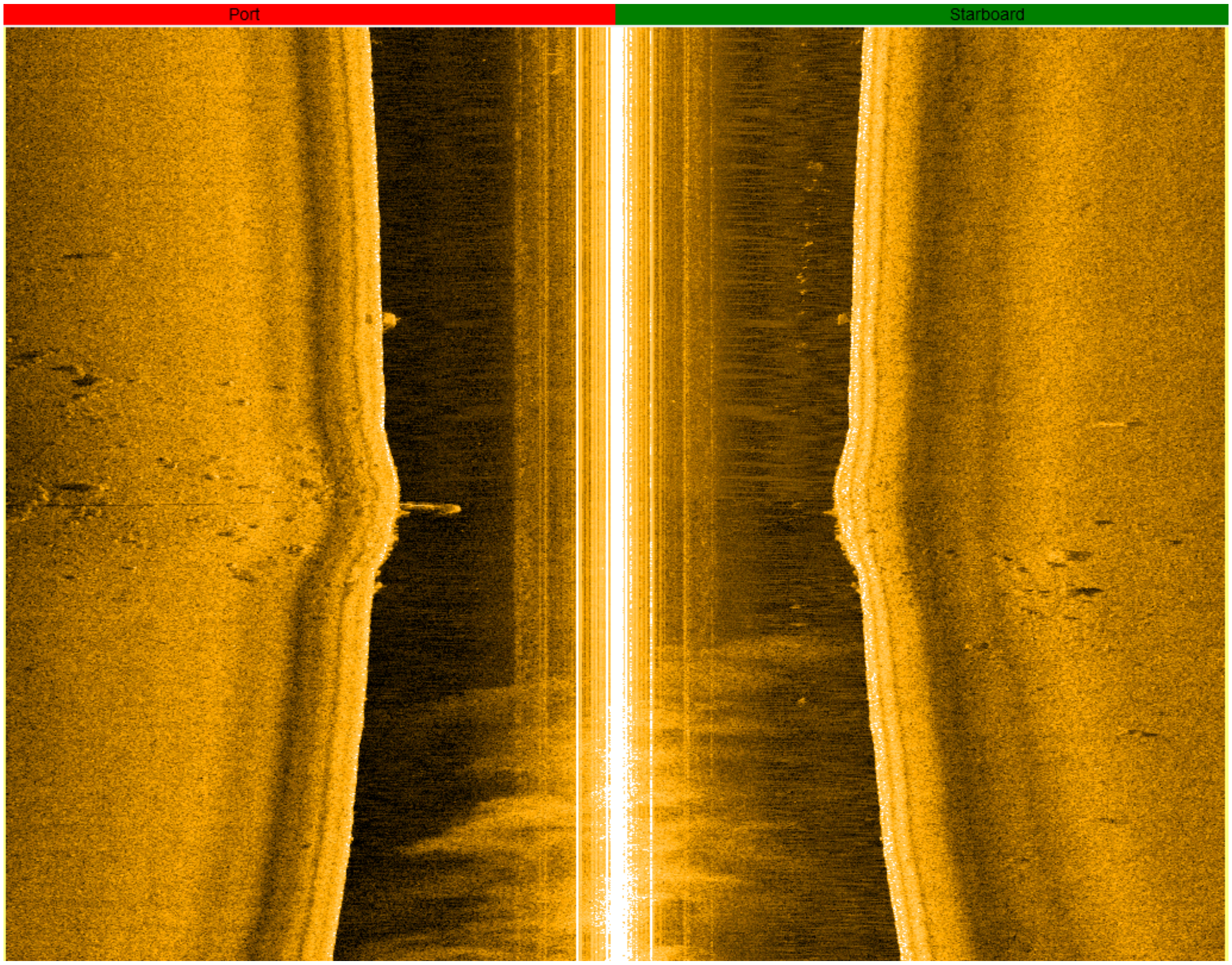


Figure 40: Waterfall view of Garmin GCV-10 sidescan record (Figure 39) with water column collected at ~4kts, 20m scan range, 800kHz, in vicinity of Stielman Rocks, Portsmouth Harbor, New Hampshire.

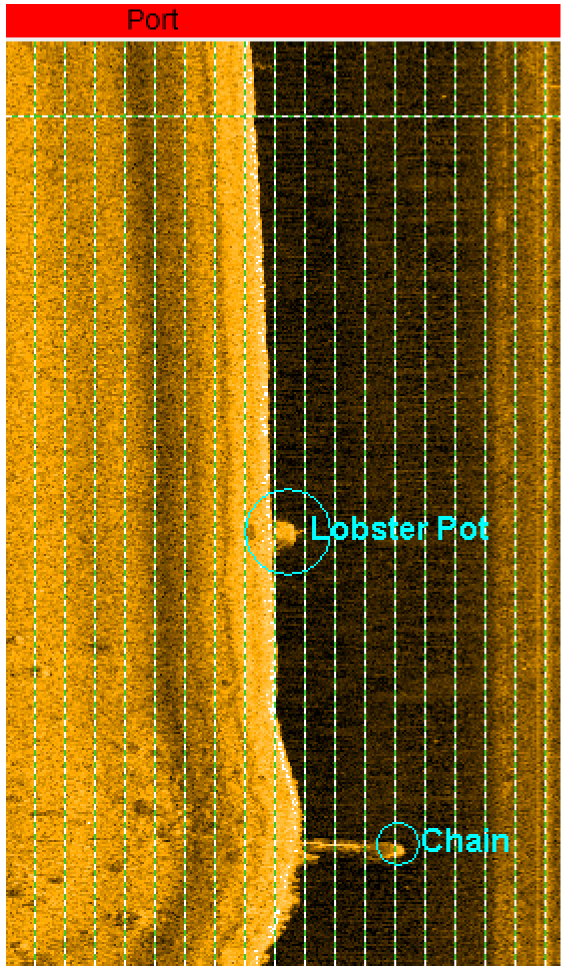


Figure 41: Zoomed in view on two targets visible in Figure 40, with horizontal scale lines at 1 meter interval starting from nadir. Notice the system's ability to image the buoy line coming off the lobster pot, and the mooring chain for USCG navigation buoy GC'3'.

The automated scan adjacent to the orange star in Figure 38, provides an example of the system's performance in a bathymetrically complex area with a variety of target sizes and morphologies (Figures 42 & 43).

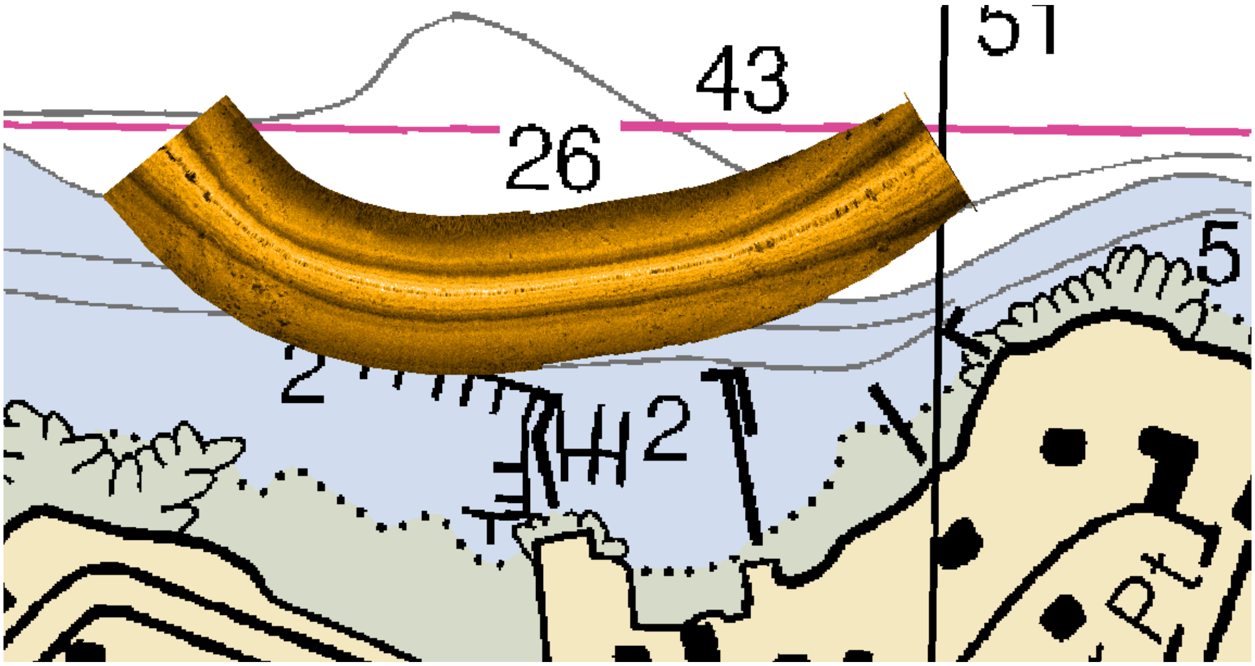


Figure 42: Georeferenced sidescan record collected at 800 kHz with 40m swath width. Overlaid on NOAA chart 13283.

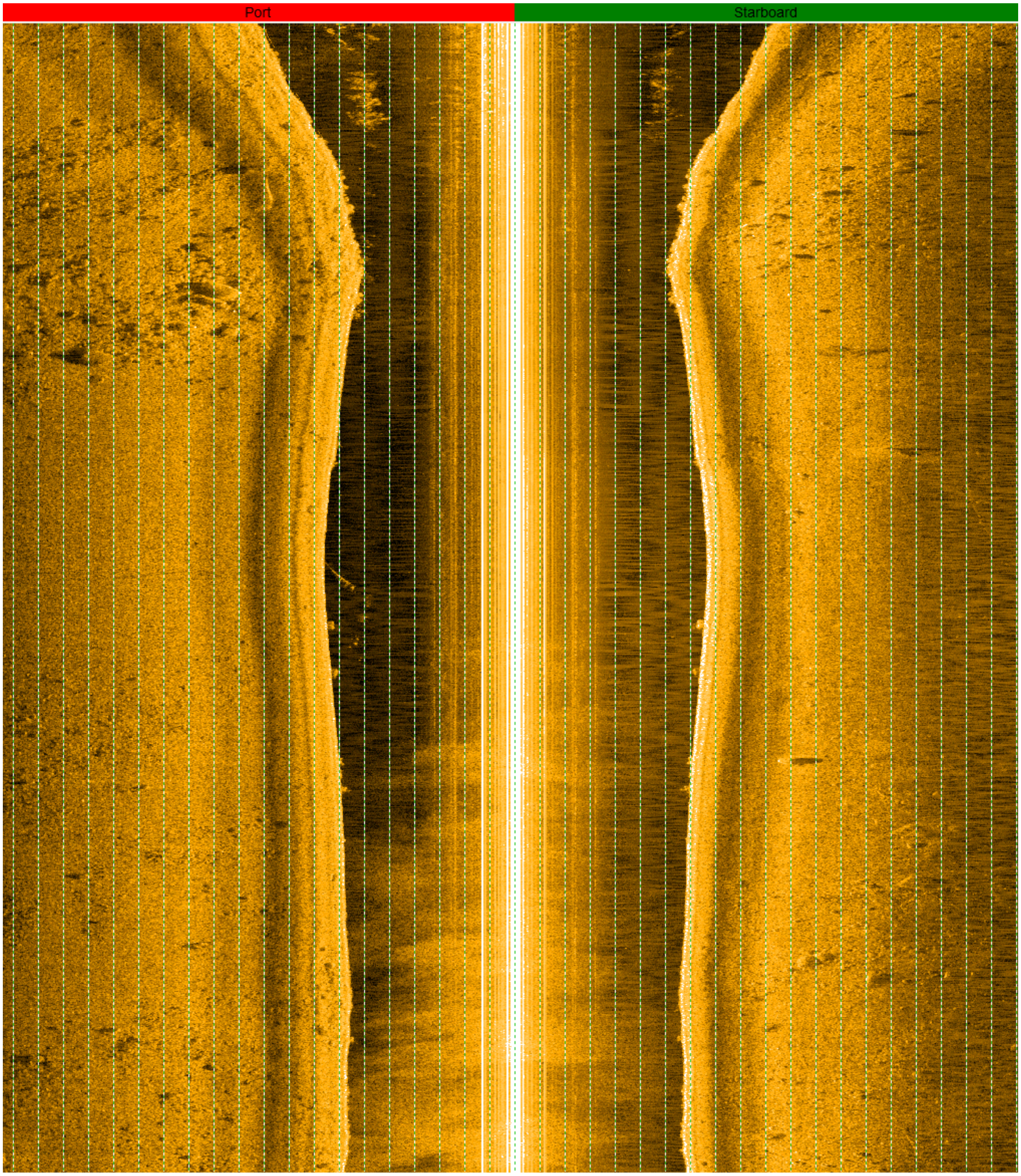


Figure 43: Waterfall view of sidescan record from Figure 42. Horizontal scale lines overlaid at 1m interval for scale.

Another automated scan of a pier facility on the Newington, New Hampshire shoreline of the Piscataqua River provides a demonstration of the horizontal positioning precision of the georeferenced sidescan imagery by allowing visual comparison of the sidescan imagery to a target's surface expression, Figure 44.

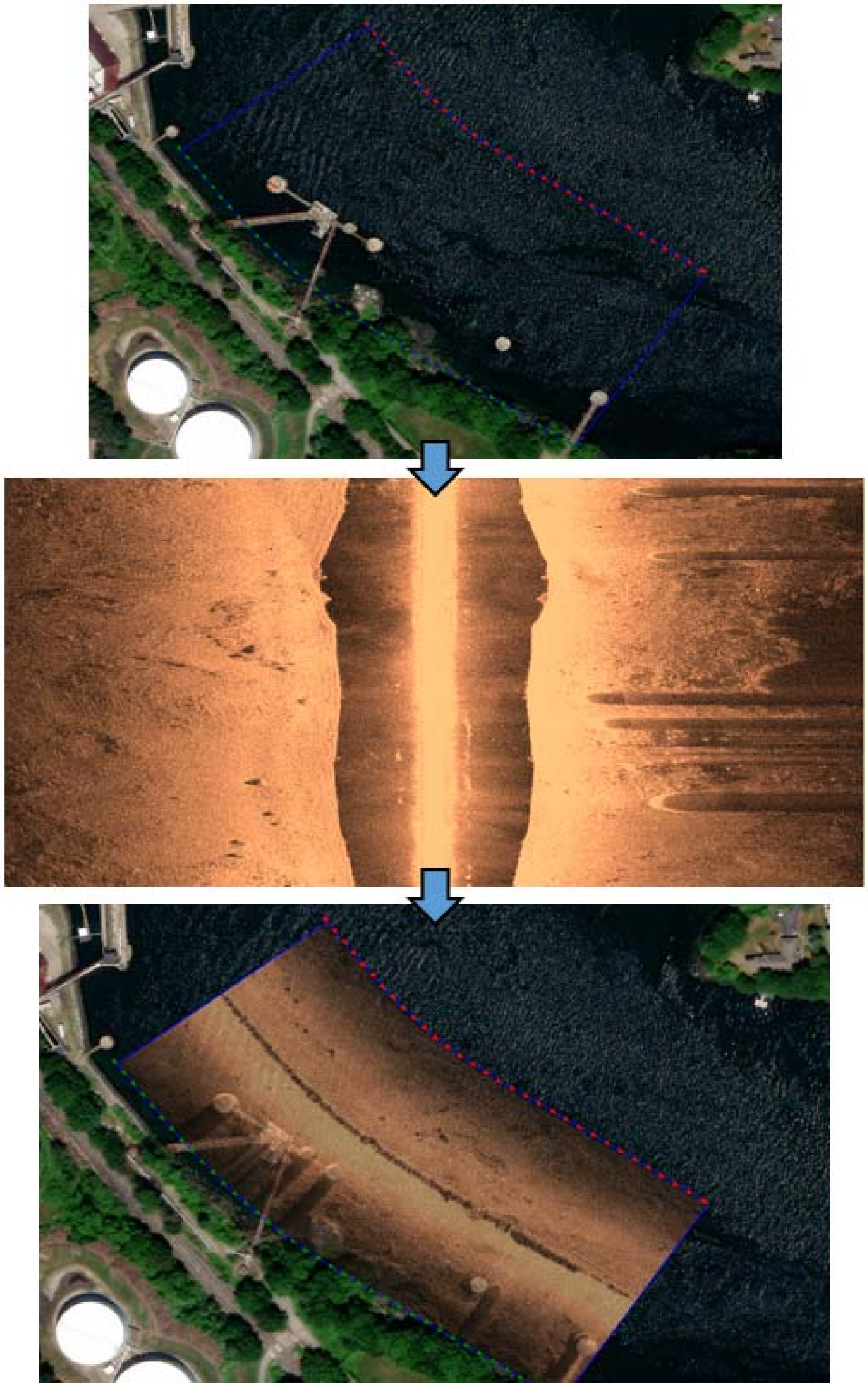

Figure 44: Post processed sidescan record collected at 6kts, 455 kHz, 70m sidescan range in the Piscataqua River, Newington, NH. Some opacity has been applied to the sidescan record for visual comparison with satellite imagery. Notice close correlation between the sidescan layer and the pilings of the main wharf. The data was collected during a strong ebb tidal flow, which induced significant vessel crabbing most visible in the offset between the satellite imagery of the lone pilings and the sidescan record.

This concept for autonomous operation demonstrates an operational model in which TCB equipped vessels may produce high quality, precisely georeferenced, sidescan images of hydrographic targets of interest with zero user input.

However, it is important to recognize that targets of interest to a HO are most likely charted at approximate positions. The model presented in this section may be easily adjusted to allow a HO to significantly expand the boundary circle around a target, or to change the shape to a more general polygon. Any boundary shape generated could be scaled to reflect the uncertainty of the position of the object being investigated, instead of scaled with water depth. The tradeoff to expanding the search area is that more data storage space on the TCB logger is consumed per scan, although this is unlikely to be a significant issue for vessels that can regularly offload data via an internet connection. For TCB vessels not constrained by data storage, it could be practical to log sidescan data continuously to increase the likelihood of finding completely unknown/unsuspected targets, which may be the most valuable information of all.

# CONCLUSIONS

## 4.1 Implications of This Work

The integration of the Harxon GPS500 antenna and Garmin GCV-10 sidescan sonar into the TCB system presented in Calder et al., 2020, represent a major advancement in TCB system capability, and a significant reduction in hardware cost. While the existing TCB system is relatively inexpensive given its capability for collecting auto-calibrated, ellipsoid referenced, single beam soundings with three dimensional uncertainties of an acceptable order to be considered for hydrographic use, its price tag (~$2000) is still likely prohibitive to mass adoption. The Harxon GPS500 antenna reduces this price tag to ~$1200 without sacrificing system performance and represents a significant step towards mass accessibility.

However, we recognize that this price point may still be prohibitive to achieving the penetration into the global fleet necessary to achieve data densities required to generate useful bathymetric products. In response, a non-authoritative system called the Wireless Inexpensive Bathymetric Datalogger (WIBL) is currently in development at CCOM. This datalogger is capable of logging NMEA depth data from a vessel's existing echosounder that can be cross calibrated against bathymetry from an authoritative system, such as a TCB logger. Prices are in flux due to global supply chain issues and chip shortages (2022), but the cost associated with producing a fully functional WIBL in volume is approximately $10. Therefore, it may be possible to significantly consolidate costs for collecting meaningful VGI by deploying only a handful of TCB systems in a geographic region and using those systems to cross calibrate data from hundreds or thousands of WIBL loggers.

The novel integration of the sidescan component of the Garmin GCV-10 is another force multiplier for deriving useful VGI for hydrographic organizations. While a sidescan sonar is fundamentally unable to provide bathymetry, this work provides numerous examples of the wide swath of high-resolution imagery they can collect. Sidescan imagery can provide the hydrographic organization with information on bathymetric features, water column targets, and substrate densities far beyond the track line of a TCB vessel and demonstrates a newfound data richness in the VGI space.

The Garmin GCV-10 is one of many sidescan-capable recreational echosounders in the ~$500 price range suitable for this application and was not chosen due to any defining characteristic. However, this work serves to demonstrate that integration with a TCB system is possible, and seeks to encourage sonar manufacturers to take part in mobilizing these sensors for scientific work.

One example of a use-case this system would be ideally suited for is managing deadhead logging programs popular in southern states. Deadhead logs are valuable hand-cut logs from old growth forests harvested during the turn of the 20$^{th}$ century which were lost when they sank to the bottom of the waterways used to transport them to the mill. The strength, rot resistance, and durability of these sunken logs make them up to ten times more valuable than conventional timber (Division of Water Resource Management, 2022). Deadhead logging programs are regulated by state agencies to provide public opportunity for recovering logs, but the agencies need an efficient means of assessing their inventory to provide fair and effective regulations. In Georgia, for example, the Department of Natural Resources developed a method of using geotagged screenshots of imagery from a recreational sidescan system to map deposits of deadhead logs and define river habitat zones that would be closed to logging (Kaeser & Litts, 2014). The system demonstrated in this thesis would greatly simplify, and expedite, this mapping operation without requiring substantial additional cost. Furthermore, it would improve the positioning quality of the georeferenced imagery and allow the agency to access the raw sonar data for deeper analysis and post processing to produce products that serve their objectives. It would also enable them to create a sidescan imagery base map that could be loaded into their chart plotter application so a vessel operator could view their position relative to a sidescan target in real-time. There are many examples like this across a variety of research, regulatory, and private industry spaces.

Consider an extension to the concept for operations presented in section 3.5.3 in which Garmin integrates a TCB extension into their standard multifunction display (chart plotter) package. As the TCB vessel goes about their normal work, the TCB extension displays several boundary circles defining hydrographic areas of interest on their chart plotter display. The visual cue reminds the coxswain of the TCB initiative and incentivizes them to adjust course to autonomously collect single beam and sidescan imagery in the appropriate areas. After the data is processed by the hydrographic organization, Garmin is rewarded with the bathymetry and sidescan imagery from the transit and can collate the data products into their chart libraries to create an exclusive extension to incentivize unit sales. This could be a valuable addition to the existing Active Captain[27] extension which already includes a feature for crowdsourcing hazard to navigation reports, analogous to Waze for boats. Fishermen are likely to have significant interest in these datasets to search for underwater structures where they may find fish.

Furthermore, a hydrographic office may display dangers discovered or rendered doubtful via TCB sidescan imagery directly on nautical chart accompanied by an official designation such as, Position Approximate (PA), Position Doubtful (PD), or Existence Doubtful (ED). These

[27] https://activecaptain.garmin.com/en-US/

designations convey that it is likely a hazard exists, and that the mariner should steer clear of an area, even though a TCB sidescan system may not be capable of positioning a hazard within the uncertainty envelope required for formal hydrographic survey data.

Especially for very remote and rapidly changing regions like the Arctic, or for emergency response situations such as marine debris mapping following a hurricane, TCB systems have the potential to be a primary source for authoritative bathymetric data. The addition of sidescan imagery to these datasets adds significant utility for habitat mapping, geological mapping, identifying water column targets, etc. In addition, this sidescan-capable TCB package would be well suited for data acquisition on uncrewed vessels due to its low cost, capability for autonomous operation, and limited power consumption.

## 4.2 Recommendations for Future Work

This thesis presents a working prototype for a hydrographically capable TCB system with autonomous sidescan imaging capability, however, there are several areas for future work to refine this concept:

**Investigate Alternate Sidescan Visualizations -** The alternate sidescan data visualizations transmitted on the Image Data Stream presented in section 2.5 may provide useful renderings for alternative use-cases or for specific hydrographic interests. For example, the raw digitized sidescan data in Viz 1 may provide a useful data source for mapping geology because it is not automatically dynamic range adjusted and could provide the opportunity to relate target impedance directly to pixel values. Alternatively, Viz 2 is automatically dynamic range adjusted to emphasize the highest impedance contrasts in the image. Therefore, it could be useful for mapping bedrock exposures, or finding a lost mooring block. Further research is required.

**Enable GCV-10 operation in auto-range mode** – In order to create a properly georeferenced sidescan record in XTF format one must know the sidescan range scale associated with each scanline collected. This was accomplished by reverse engineering the command to apply the appropriate sidescan range setting based on the water depth in each hydrographic area of interest. However, for most situations, it would be just as effective to command the sidescan to run in auto-range mode, and to have a mechanism to reverse-engineer the range scale associated with each datagram. Then, the range scale associated with each reassembled scanline could be programmatically included in the XTF file and the sidescan swath width would always be properly rendered.

**Integrate heading corrections** – The TCB datalogger is capable of recording data from a vessel's heading sensor in the form of NMEA heading sentences. Since recreational sidescan units, such as the Garmin GCV-10, are meant to be mounted rigidly to the vessel hull, heading error artifacts in the sidescan imagery could be corrected with the recorded vessel heading data. Therefore, offsets between the sidescan sensor's course over ground and the direction of vessel motion, which are often caused by strong wind or current, could be corrected in post processing. Heading data could also be generated directly by the TCB system by connecting a second antenna to the dual GNSS receiver board and establishing a baseline to create a "GNSS compass".

**Reverse engineer bathymetry access**- The Garmin GCV-10 has an integrated single beam capability that provides depths below the transducer. These depth measurements are transmitted for display on a topside unit via a proprietary network protocol. Reverse engineering this protocol to extract the declared depth could provide a dataset that could be used to automatically remove the water column gap in the raw sidescan data. This could enable automated data processing to create a georeferenced sidescan imagery mosaic.

**Integrate the temperature sensor** – Many recreational echosounders, including the Garmin GCV-10, include a temperature sensor integrated into the transducer housing. Water temperature is a critical factor in determining sound speed and could be used to make crude corrections for acoustic refraction artifacts in real time. This data could be used to provide slant range corrections for the sidescan system, or to reduce vertical uncertainty in the bathymetry. These corrections would be especially valuable in shallow, nearshore waters, where sound speed changes occur rapidly due to freshwater mixing and strong temperature gradients exist near the surface.

**Create a latency function-** The results of section 3.4 show that system latency likely has some dependence on sidescan range scale (+/- 0.05s). However, the magnitude of horizontal sounding uncertainty associated with the uncertainty in latency estimation is small, on the order of 10-20cm at 4 or 8 knots respectively. Regardless, future work could test system latency more stringently, at a wider variety of range scales, and implement a function that adjusts system latency compensation according to the precise range setting the data was collected at. This work may be especially valuable in minimizing latency artifacts visible in mosaicked sidescan imagery.

# List of References

Calder, B. R., Dijkstra, S. J., Hoy, S., Himschoot, K., & Schofield, A. (2020). A Design for a Trusted Community Bathymetry System. *Marine Geodesy*, 1-32.

C. Noll, The Crustal Dynamics Data Information System: A resource to support scientific analysis using space geodesy, Advances in Space Research, Volume 45, Issue 12, 15 June 2010, Pages 1421-1440, ISSN 0273-1177, DOI: 10.1016/j.asr.2010.01.018.

Division of Water Resource Management. "Deadhead Logging." *Florida Department of Environmental Protection*, Submerged Lands and Environmental Resources Coordination Program, 6 Oct. 2022, https://floridadep.gov/water/submerged-lands-environmental-resources-coordination/content/deadhead-logging.

GEBCO (2022, June 29). *Mapping Progress*. The Nippon Foundation-GEBCO Seabed 2030 Project. Retrieved January 26, 2022, from https://seabed2030.org/mapping-progress

Howe, J. (2008). "Crowd Sourcing: Why the Power of the Crowd is Driving the Future of Business", Crown Business (Random House), New York (eISBN: 978-0-307-44932-0, v3.0)

Hoy, S., and B. Calder (2019). "The Viability of Crowd-source Bathymetry for Authoritative Purposes". Proc. U.S. Hydrographic Conference, Biloxi, MS.

Hughes Clarke, John. "Conventional and Focused Sidescans ." OE/ESCI 874 Ocean Mapping 1. 5 Oct. 2016.

IHO. Crowdsourced Bathymetry. Retrieved on January 20, 2020. Retrieved from: https://iho.int/en/crowdsourced-bathymetry James, M. R. & Robson, S. (2014). Mitigating systematic error in topographic models

International Hydrographic Organization (2008) IHO Standards for Hydrographic Surveys, 5th edition, February 2008. Monaco, International Hydrographic Bureau, 28pp. (International Hydrographic Organization Special Publication, S-44). DOI: http://dx.doi.org/10.25607/OBP-1354

Kaeser, Adam & Litts, Thomas. (2014). An Illustrated Guide to Low-Cost Sonar Habitat Mapping v1.0.

Mayer, L., Jakobsson, M., Allen, G., Dorschel, B., Falconer, R., Ferrini, V., Lamarche, G., Snaith, H., & Weatherall, P. (2018). The Nippon Foundation—GEBCO seabed 2030 project: The quest to see the world's oceans completely mapped by 2030. *Geosciences*, 8(2), 63.
NGS. National Geodetic Survey Data Explorer

Mills, D. (1992) “Network time protocol (version 3): Specification, implementation and analysis,” Internet Engineering Task Force, [online: http://www.rfcs.org], Tech. Rep. RFC-1305.

O’Heran, C., Calder, B. (2021) Horizontal Calibration of Vessels with UASs, Marine Geodesy, 44:2, 91-107, DOI: 10.1080/01490419.2021.1879330

Rondeau, Mathieu. (2019). Bad Information Is Better Than No Information At All - Assessing the uncertainty of bathymetric collaborative data collected with a HydroBox system. 10.13140/RG.2.2.34784.10243.

Rondeau, Mathieu & Seube, Nicolas & Deunf, Julian. (2016). Surveying in Hostile and Non Accessible Areas with the Bathymetric HydroBall® Buoy. 10.1007/978-3-319-32107-3_5.

T.Takasu, RTKLIB: Open Source Program Package for RTK-GPS, FOSS4G 2009 Tokyo, Japan, November 2, 2009

Tozer, B, Sandwell, D. T., Smith, W. H. F., Olson, C., Beale, J. R., & Wessel, P. (2019). Global bathymetry and topography at 15 arc sec:SRTM15+. Earth and Space Science, 6, 1847– 1864. https://doi.org/10.1029/2019EA000658

Tuexen, Michael, et al. “PCAP Next Generation (Pcapng) Capture File Format.” *PCAP next Generation (Pcapng) Capture File Format*, Network Working Group, 23 June 2021, https://www.ietf.org/archive/id/draft-tuexen-opsawg-pcapng-03.html#name-references.

# APPENDIX A

## Table of Software

| Name | Producer | Description | Link |
|---|---|---|---|
| **pyxtf 1.2** | Oystein Sture | Open-Source eXtended Triton Format (XTF) file interface | https://github.com/oysstu/pyxtf |
| **XTF Converter** | Daniel Tauriello | Custom adaptation of pyxtf 1.2 | https://bitbucket.org/dtauriello/tcb_sidescan/src/main/XTF%20Converter/ |
| **SonarWiz** | Chesapeake Technology | Complete Hydrographic Software Package | https://chesapeaketech.com/products/sonarwiz-sidescan/ |
| **Hypack** | Xylem | Complete Hydrographic Software Package | https://www.hypack.com/ |
| **Wireshark** | The Wireshark Team | Open-Source Network Protocol Analyzer | https://www.wireshark.org/ |
| **Plotsinglesolutions.m** | Daniel Tauriello | Custom MATLAB Code | https://bitbucket.org/dtauriello/tcb_sidescan/src/main/plotsinglesolutions.m |
| **GCV-10 Commands** | Daniel Tauriello | Custom Python Code | https://bitbucket.org/dtauriello/tcb_sidescan/src/main/GCV-10%20Commands/ |
| **PARSER_basic.m** | Daniel Tauriello | Custom MATLAB Code | https://bitbucket.org/dtauriello/tcb_sidescan/src/main/Basic%20Datagram%20Parser/PARSER_basic.m |
| **xtf_converter_TCB.py** | Daniel Tauriello | Custom Python Code | https://bitbucket.org/dtauriello/tcb_sidescan/src/main/XTF%20Converter/xtf_converter_TCB.py |
| **PARSER_master.m** | Daniel Tauriello | Custom MATLAB Code | https://bitbucket.org/dtauriello/tcb_sidescan/src/main/RVGSTest_03102021/PARSER_Master.m |
| **monitor_realtime_position.py** | Daniel Tauriello | Custom Python Code | https://bitbucket.org/dtauriello/tcb_sidescan/src/main/monitor_realtime_postition.py |

# Data Volume Experiment

The Garmin GCV-10 was mobilized on R/V Gulf Surveyor and controlled using a Garmin GPSMAP 742XS chart plotter. A LAN tap[28] was installed between the echosounder processor and chart plotter to allow a laptop running Wireshark[29] to log all traffic between the two devices. The side-scan traffic was filtered out of the data stream using Wireshark's built-in packet filtering functions. Side-scan data was collected in 455kHz CHIRP mode, and the device was set to automatically adjust the range setting based on water depth. It was observed that the range is automatically adjusted to approximately 3x water depth below transducer. Data volumes are between 6-12MB/minute at depths between 0-50m (range setting < 150m) and fall to 2-5MB/minute in depths greater than 50m (range setting > 50m). Therefore, if the system is operated in very shallow water and acquires side-scan data at the maximum rate of 12MB/minute it will take almost 1.5 hours to fill 1GB of drive space on the data logger.

[28] Throwing star LAN Tap: https://greatscottgadgets.com/throwingstar/

[29] Wireshark is a network protocol analyzer. It can be found at wireshark.org

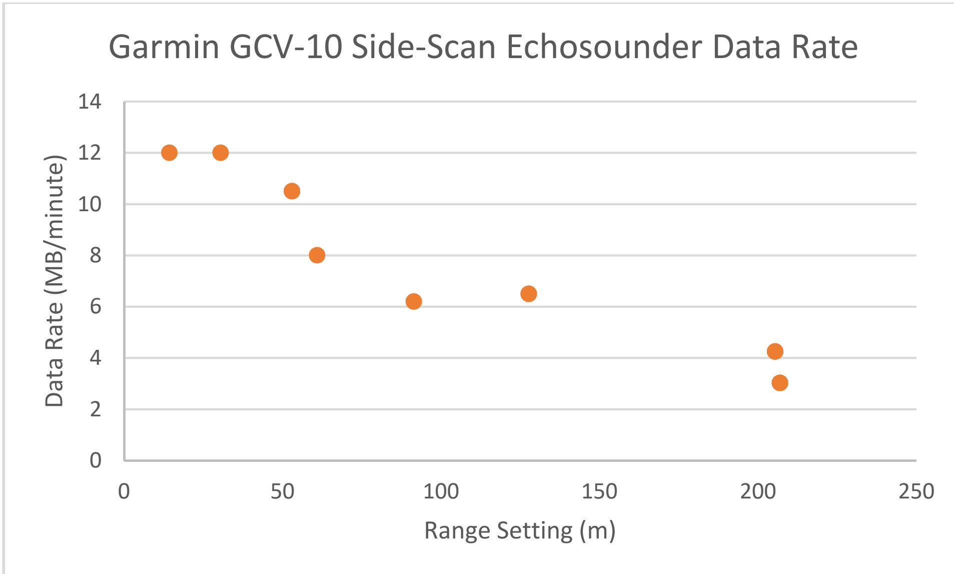


Figure 45: Range is the distance from nadir to one edge of the side-scan swath. Effectively half the total swath width. It's likely that changes in ping rate account for changes in data volume but proving that relationship was outside the scope of this project.

# APPENDIX B

## Logging Side Scan Data with the TCB Datalogger

### Physical Installation

Connect to an open network port on the GCV-10 with a standard Ethernet patch cable rated to minimum 100Mbps throughput.

## Software Installation

Tshark[30] -- a lightweight network packet capture and analysis program that runs under a command line interface was installed on the TCB datalogger. This program includes a network traffic dump tool called, Dumpcap[31], which allows the user to filter and capture data from a live network and write the packets to file. Dumpcap can be installed by connecting the Odroid C2 to the internet, and then executing:

**sudo apt-get install tshark**

## Echosounder Data Capture

The following command uses Dumpcap to filter and capture UDP datagrams containing sidescan imagery from the **Image Data Stream** in real-time:

**dumpcap –i 1 –q –b filesize:200000 –b files:50 –f "host 172.16.3.196 and udp port 50220" –w /root/dumpcap_captures**

**-i:** defines capture interface on the TCB datalogger.

**-q:** enable quiet mode

**-b:** ring buffer. With the ring buffer enabled, dumpcap will capture data until the defined file size is reached, and then automatically create a new file.

**filesize:** defined in KiB. Therefore filesize: 200000 will collect a 200MB file before a new file is created. A 200MB file contains approximately 10 minutes of side scan imagery.

**Files:** defines how many files can be written before the system begins overwriting data. In this example files:50 would allow you collect 50x200= 10,000MB or 10GB of data. This number can be adjusted to reflect the amount of free space available on the datalogger's SD card.

**-f** defines the capture filter to isolate the **Image Data Stream**

[30] Tshark manual page: https://www.wireshark.org/docs/man-pages/tshark.html

[31] Dumpcap manual page: https://www.wireshark.org/docs/man-pages/dumpcap.html

**-w** write captured files to a directory

# Desktop Latency Experiment Procedure

1. Apply the following sonar settings to maximize the visibility of a finger tap on the transducer face in the sidescan record:
   a. Frequency: 455kHz Chirp
   b. Scroll Speed: Fast
   c. Brightness: Auto Medium
   d. Appearance color scheme: Midnight Blue
   e. Leave all other settings default.
2. Set the Odroid's NIC to 192.168.2.117 to establish an internet connection to install RPi.GPIO.
3. Install the GPIO library at /wiringPi/RPi.GPIO-ODROID/test

   In that directory you'll find latency_test.py which logs its output to latency_triggers.txt, a simple text file which holds the timestamps from when the circuit is completed by touching the wire to the bare wire stuck on the outside of the transducer.
1. Install TShark (includes dumpcap). TShark is a network protocol analyzer which allows live packet capture from the **Image Data Stream**:

   **Sudo apt-get update**

   **Sudo apt-get install tshark**
2. The experiment stores files in two places:
   a. Dumpcap capture files are stored in /root/dumpcap_captures
   b. Text file reporting status of interrupt circuit in /root/wiringpi/RPi.GPIO.Odroid/test
3. Make sure the system date is correct, and you are logging GNSS observations.
4. Clear the above directories of old data files if you want to prevent confusion.
5. Navigate to location of latency_test.py script that monitors the interrupt circuit:

   **cd/root/wiringpi/RPi.GPIO.Odroid/test**
6. Start transmitting on the sonar at a manual range setting of your choice. Capture UDP packets containing sidescan image data and filter out extraneous traffic using:

**dumpcap –i 1 –q –b filesize:200000 –b files:50 –f "host 172.16.3.196 and udp port 50220 and len>=1000" –w /root/dumpcap_captures**

7. ctrl-z to pause capture, then **bg** to continue executing dumpcap process in background
8. Run the latency test python script:

   **sudo python3 latency_test.py**

9. Press index finger down on the wire, momentarily covering one transducer stave on while simultaneously completing interrupt circuit. A quick, even, cover of one transducer stave (with the other side face down on the table) will show a bright scanline on the display.

   Ctrl-z to stop latency test script

10. Stop dumpcap packet capture:

    **pkill dumpcap**

11. The latency test script logs the circuit status to a text file called triggers.txt, when the circuit is closed it prints the system interrupt time, rename it to save the data from the current run:

    **mv triggers.txt newname.txt**

## Processing Desktop Latency Experiment Data:

1. Use Cyberduck to ftp files off the datalogger.
2. Run tshark.m script to follow udp stream and export data payload as "raw" for each dumpcap capture. Follow instructions in the script.
3. Open Import_Data.m script and update input variables. (Copy all paths to processed captures by sorting by file type in Program Files\Wireshark and shift+rt click copy as path)
4. Rip packet number and time out of dumpcap captures and import to matlab:
   1. Copy all the commands from the tshark.txt script and paste into Excel.
   2. Data> Text to Columns > Delimited> Space>Format as Text
   3. Delete columns D,E,F then add a column on either side of the path with just "
   4. Use =Cellx&CellY to concatenate '"' on both sides of the path.
      a. Example of the command, writing capture timestamps to 36.csv (range setting 3m, run #6):

tshark -r "C:\Users\Field\Desktop\latency 4.29.20\36_00001_20200501135656" -tu > 36.csv

   5. Use the Text to Columns with a "." Delimiter on just the filename.txt column to strip out .txt and insert .csv
   6. Select all and copy paste it to a notepad file. Save it as a .txt file and as a .cmd file.
   7. Put the .cmd file in C:\ProgramFiles\Wireshark *** Note windows doesn't allow you to save directly to program files so you must save to some other directory first, then copy paste to program files**
   8. Open command prompt, navigate to C:\ProgramFiles\Wireshark and execute the script. Copy all the .csv files to your MATLAB working directory.
   9. Update and run importdumpcaptimestamps_master.m

5. Run PARSER_latency05052020.m
    a. Define file, trig, and dumpcaptime for the run you want to evaluate.
        i. File name scheme: 31,32,33 are runs 1,2&3 of 3m range setting, 20020 is run 20 of 200m range setting
        ii. Import all runs associated with a single range setting to MATLAB
6. The PARSER script picks out the scanline with the highest average value over the line's last 500 bytes. This successfully picks out the first line when the finger tap was detected if the detection was only 1 scanline long.

## Processing Data from Field Collection

An example dataset from sidescan collection on 03/10/2021 is available here:

https://bitbucket.org/dtauriello/tcb_sidescan/src/main/RVGSTest_03102021/

At the time this data was processed the tool, RTKGet, which is part of the RTKLib software did not work because the Crustal Dynamics Data Information System (CDDIS) discontinued authentication free FTP access. You must create a free account to access the FTP site.

1. Launch RTKLIB via RTKLaunch.exe

2. Manually download RINEX navigation file (.xxn) from here: https://cddis.nasa.gov/archive/gnss/data/daily/2021/

The directories are organized by Julian day. Find the BRDC file inside the XXn directory

3. Download ephemerides and clock correction data (.sp3) from here: https://cddis.nasa.gov/archive/gnss/products/2143/

4. Get the precise ionospheric data (.xxi) here: https://cddis.nasa.gov/archive/gnss/products/ionex/2021/

    The directories are organized by day number so Feb 10, 2021, is day '041'.

5. Get the rinex data for the NHUN CORS control point, and the station coordinates:

    https://geodesy.noaa.gov/CORS/standard1.shtml

    Convert NHUN coordinates using the MATLAB script coordtransform.m and input corrected coordinates on the Positions tab of RTKPost.

6. Set RTKPost options menus as follows:

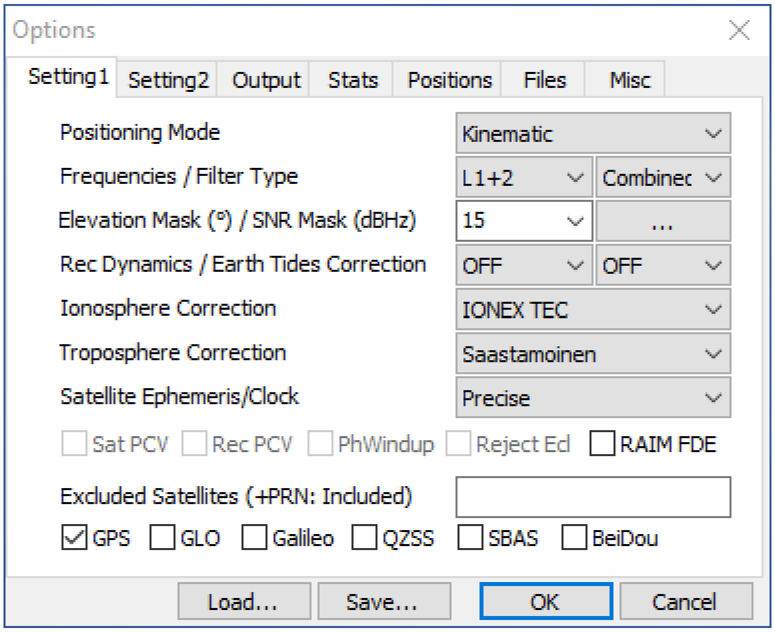


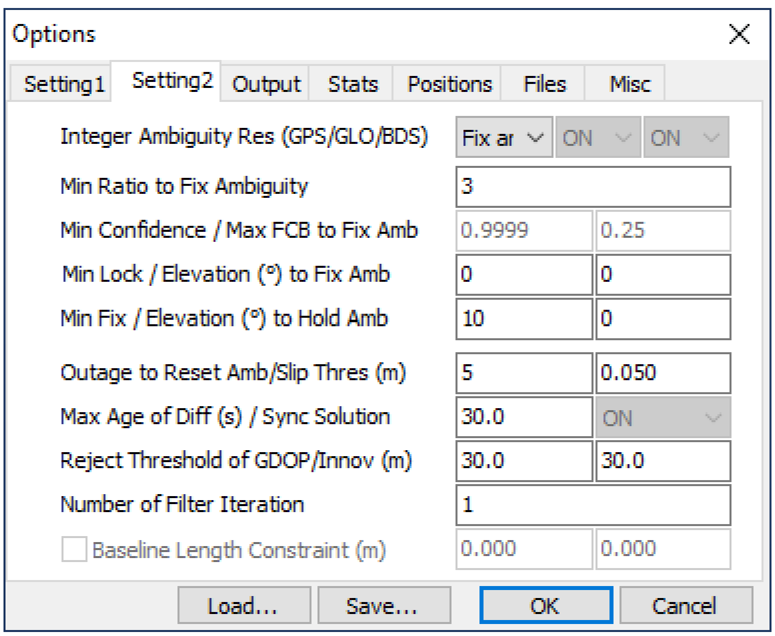

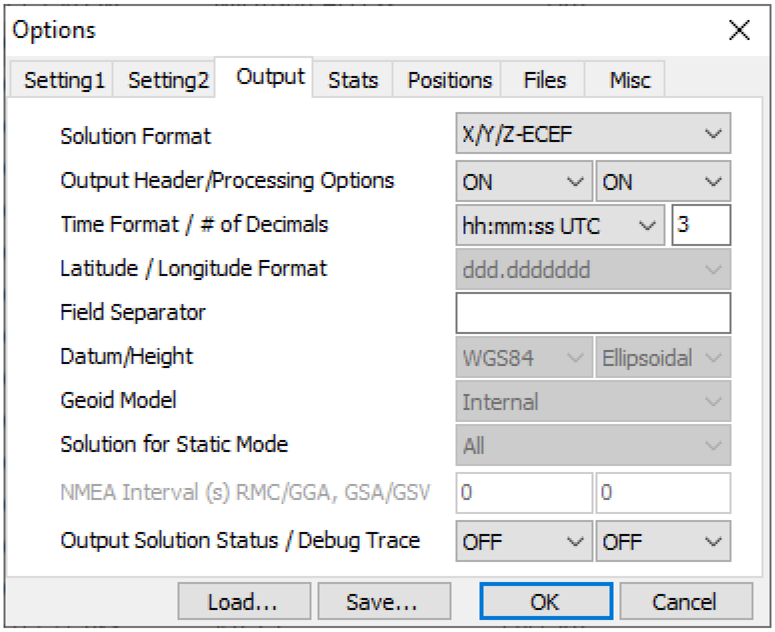


***Make sure Time Format is UTC!

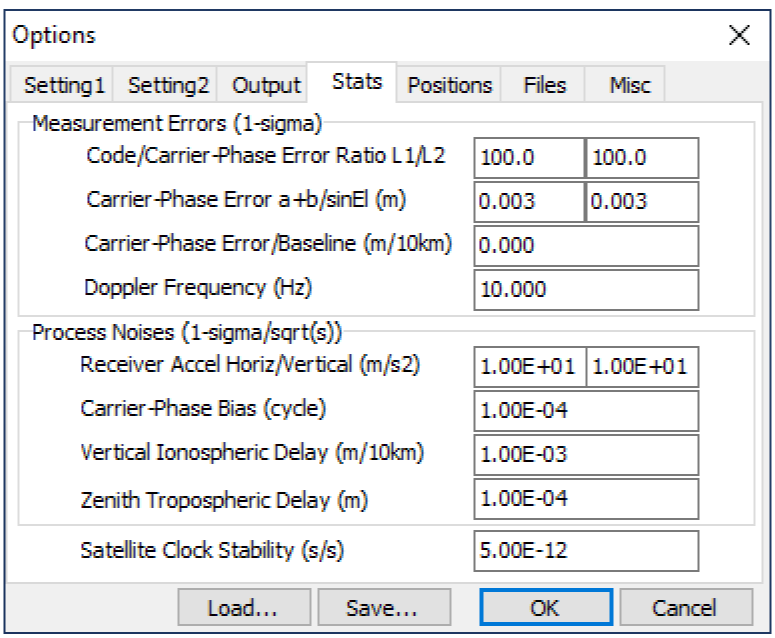

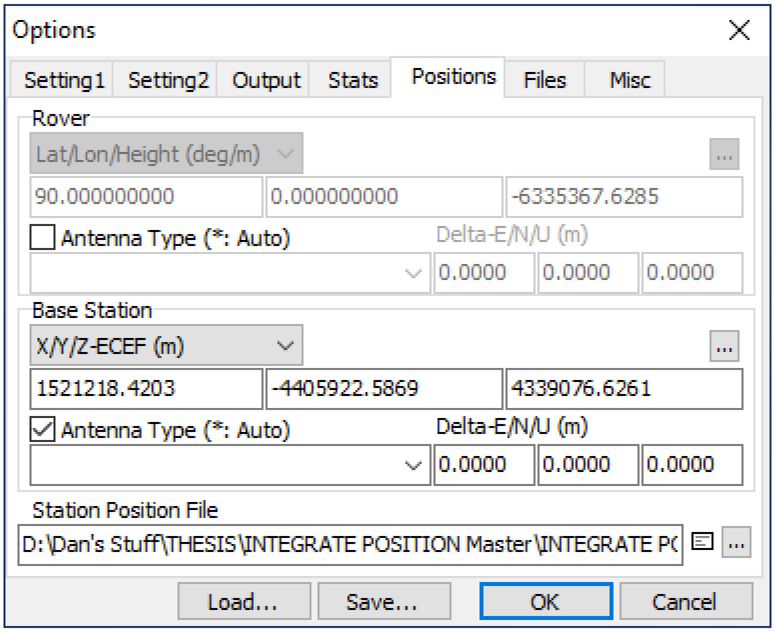


7. Open the tshark.m script and follow the instructions.
8. Run MATLAB script PARSER_Master_Input.m
9. This rewards you with and .xtf file for each dumpcap capture file. The XTF files will have the properties in xtf_converter_DT_master.py embedded into them. Most importantly, you define the sidescan range setting and frequency setting during data acquisition, in this script. Adjust these and reprocesses so that you have a version of each capture processed with the correct range and frequency setting.
10. Open **SonarWiz** and let the wizard import the Geodesy settings from the XTF file. Optionally enter horizontal (XY) offset from antenna to sidescan transducer as a sheave offset in the Sonar File Manager to decrease horizontal positioning uncertainty.

a. Define the samples per channel (The GCV-10 collects 2048 samples on each stave for each ping)

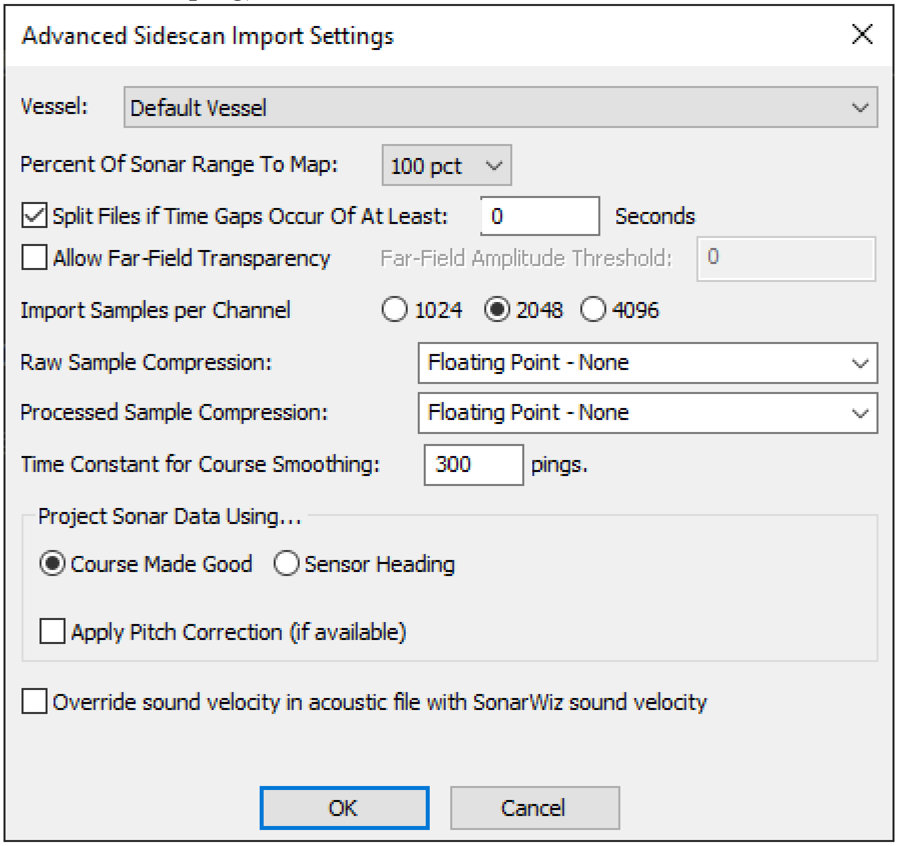


b. Load the XTF file into a compatible hydrographic software program.